RSC Medicinal Chemistry

ROYAL SOCIETY OF CHEMISTRY

RESEARCH ARTICLE

Cite this: *RSC Med. Chem.*, 2022, **13**, 413

Structure–activity relationships of hydrophobic alkyl acrylamides as tissue transglutaminase inhibitors†

Alana M. M. Rangaswamy, Pauline Navals, Eric W. J. Gates, Sammir Shad, Sarah K. I. Watt and Jeffrey W. Keillor *

Received 2nd December 2021,
Accepted 25th January 2022

DOI: 10.1039/d1md00382h

rsc.li/medchem

Tissue transglutaminase (TG2) is a multifunctional protein that plays biological roles based on its ability to catalyse protein cross-linking and to function as a non-canonical G-protein known as Ghα. The non-regulated activity of TG2 has been implicated in fibrosis, celiac disease and the survival of cancer stem cells, underpinning the therapeutic potential of cell permeable small molecule inhibitors of TG2. In the current study, we designed a small library of inhibitors to explore the importance of a terminal hydrophobic moiety, as well as the length of the tether to the irreversible acrylamide warhead. Subsequent kinetic evaluation using an *in vitro* activity assay provided values for the k_{inact} and K_I parameters for each of these irreversible inhibitors. The resulting structure–activity relationship (SAR) clearly indicated the affinity conferred by dansyl and adamantyl moieties, as well as the efficiency provided by the shortest warhead tether. We also provide the first direct evidence of the capability of these inhibitors to suppress the GTP binding ability of TG2, at least partially. However, it is intriguing to note that the SAR trends observed herein are opposite to those predicted by molecular modelling – namely that longer tether groups should improve binding affinity by allowing for deeper insertion of the hydrophobic moiety into a hydrophobic pocket on the enzyme. This discrepancy leads us to question whether the existing crystallographic structures of TG2 are appropriate for docking non-peptidic inhibitors. In the absence of a more relevant crystallographic structure, the data from rigorous kinetic studies, such as those provided herein, are critically important for the development of future small molecule TG2 inhibitors.

Introduction

Transglutaminases are a family of calcium-dependent enzymes known for their ability to cross-link proteins through formation of an N^{ε}(γ-glutaminyl)lysine bond.[1–3] These enzymes catalyze the formation of this covalent bond by mediating an acyl transfer mechanism through their active site cysteine residue.[4,5] Transglutaminase 2 (TG2) is the most intensively studied isozyme of the transglutaminase family and has been implicated in fibrosis,[6–8] celiac disease,[9,10] and cancer metastasis.[11–13] TG2 distinguishes itself from the other transglutaminases in that it also plays the role of an intracellular G-protein, in which it is known as Ghα.[14] The TG2 protein undergoes a dramatic conformational change allowing its mutually exclusive function as either a G-protein, or as a cross-linking enzyme.[15] When it adopts an open, linear, conformation that is stabilized by the binding of calcium ions, the transamidase binding site is formed, where substrates can bind before being crosslinked, isopeptidically cleaved, or hydrolysed.[16] However, TG2 can also adopt a more compact, closed, form where its two C-terminal β-barrels fold in to cover the catalytic core, abolishing the transamidase binding site, and forming a GTP binding site that allows its G-protein activity.[14] These two activities are mutually exclusive, with each conformation lacking the binding site for the opposing substrate.[14,16–18]

Extensive work has gone in to validating TG2 as a therapeutic target in the treatment of celiac disease, cancer, and kidney fibrosis.[19] Inhibitors of TG2 are extremely diverse, ranging from small molecules[20–22] to peptides.[23,24] Many of these inhibitors are designed to inactivate TG2's transamidase activity irreversibly, while some are also designed to suppress GTP binding by locking the enzyme in its open conformation.[25] Since the first structure of the open conformation of TG2 was determined through X-ray crystallography,[16] a hydrophobic pocket has been identified in the transamidase binding site on the α/β-catalytic core.

Department of Chemistry and Biomolecular Sciences, University of Ottawa, Ottawa, Ontario K1N 6N5, Canada. E-mail: jkeillor@uottawa.ca

† Electronic supplementary information (ESI) available: Computational modelling details; HPLC retention times and analysis of purity for all final compounds; and ^{1}H and ^{13}C NMR spectra for all final compounds. See DOI: 10.1039/d1md00382h

This pocket, sometimes referred to as the 'D-site', is very appealing for the design of high affinity inhibitors. The scaffolds of many inhibitors have been designed to allow binding in the D-site, while presenting an electrophilic group that can react with the catalytic cysteine in the active site tunnel. These warhead groups include acrylamides,[21,22,26,27] epoxides,[28] 6-diazo-5-oxo-norleucine (DON),[10] and other α,β-unsaturated carbonyl groups.[24,29] Very recently, peptidomimetic inhibitors designed to inhibit intestinal TG2 have progressed through phase II clinical trials for the treatment of celiac disease.[30] However, there still remains a need for inhibitors of intracellular TG2, particularly in the context of its role in cancer, for which cell permeability is a critical hurdle.

In our previous work, we designed targeted covalent inhibitors of TG2 that were originally designed to mimic the structure of the glutamine substrate Cbz-Gln-Gly.[24,26,28,29,31–33] These peptidomimetic inhibitors were subsequently optimized through multiple structure activity relationship (SAR) studies, resulting in inhibitors that are highly efficient and selective for TG2. The latest generations bear an acrylamide warhead that reacts with the active site cysteine, while filling the D-site pocket with a naphthoyl group (*e.g.*, AA9) or a dansyl group (*e.g.* VA4) attached to a piperazine linker (Fig. 1).[26]

Taking an alternative approach, both the Cure Huntington's Disease Initiative Foundation (CHDI) and the Griffin group have developed small molecule inhibitors of TG2 through structure-based design.[21,22,34,35] It is noteworthy that some of the most efficient inhibitors originating from this structure-based design also include piperazine-linked hydrophobic groups. This suggests that three research groups independently converged on a structural feature that confers affinity and favours binding, potentially by directing a hydrophobic group to the TG2 D-site. We were particularly intrigued by the lead compound developed by Badarau *et al.*, featuring a dansyl fluorophore, piperazine bridge, and glycine linker to the acrylamide warhead, referred to as 3h in the original article,[21] but also known as EB-1-155 (ref. 34) (Fig. 1). This inhibitor bears the same piperazine-dansyl motif as our inhibitor VA4; however, it is striking to note that although EB-1-155 lacks all of the structural elements of the N-terminus of VA4, this is not detrimental to potency, selectivity, or GTP binding suppression. This led us to hypothesize that directing a hydrophobic group to the D-site is of primary importance in the design of TG2 inhibitors and inspired us to design a simple SAR study to test this hypothesis. In the current work we varied both the hydrophobic moiety on the piperazine, and the length of the chain bearing the acrylamide warhead, seeking to find the ideal arrangement for optimizing D-site binding affinity. We evaluated the efficiency of these novel inhibitors[36] and their ability to suppress GTP binding,[37] and compare these data to the binding modes predicted by molecular modelling.

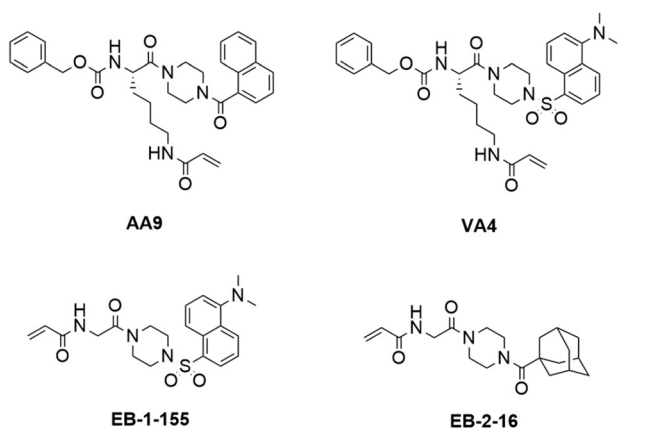

Fig. 1 Structures of previously disclosed TG2 targeted covalent inhibitors. Peptidomimetic inhibitors AA9 and VA4 from the Keillor group[26] and small molecule inhibitors EB-2-16 and EB-1-155 from the Griffin group.[21,34]

Results and discussion

Design

The structure-based design of TG2 inhibitors has been greatly enabled by the publication of the first crystallographic structure of the open conformation of the enzyme.[16] This structure was obtained after reaction of the enzyme with a peptidic irreversible inhibitor, and arguably represents the structure of the transamidase-active enzyme, or its acyl–enzyme intermediate. As identified by the original authors, the surface of the open conformation of TG2 features a distinctive hydrophobic pocket, several angstroms away from the mouth of the tunnel leading down to the active site cysteine residue, CYS277. Our primary design criteria were to fill this hydrophobic pocket with a small series of ligands attached to a central piperazine scaffold, and to vary the length of the pendant tether to which a terminal acrylamide warhead was attached. Our initial choice of hydrophobic moieties included three that were previously observed to confer affinity to other series of inhibitors, namely, the adamantyl group identified[21] by Badarau *et al.*, the naphthyl group identified[26] by Akbar *et al.*, and the dansyl group studied by both research groups (Fig. 1).[21,26] For the tether length, we chose to vary the number of methylene units from n = 1, studied by Badarau *et al.*, to n = 5, resembling the peptidomimetic scaffold used by Akbar *et al.*[21,26]

Synthesis

The synthesis of inhibitors **22–25(a–e)** was performed according to the route shown in Scheme 1. Compounds **6–9** were prepared through functionalization of Boc-piperazine with a hydrophobic group (dansyl, naphthoyl, adamantanecarbonyl, or naphthalenesulfonyl) *via* the commercially available acyl- or sulfonyl chlorides (**3–5**), except for adamantanecarbonyl chloride (**2**) which was prepared from the corresponding carboxylic acid. Deprotection of the piperazinyl Boc group was performed under acidic conditions: although it is common to perform

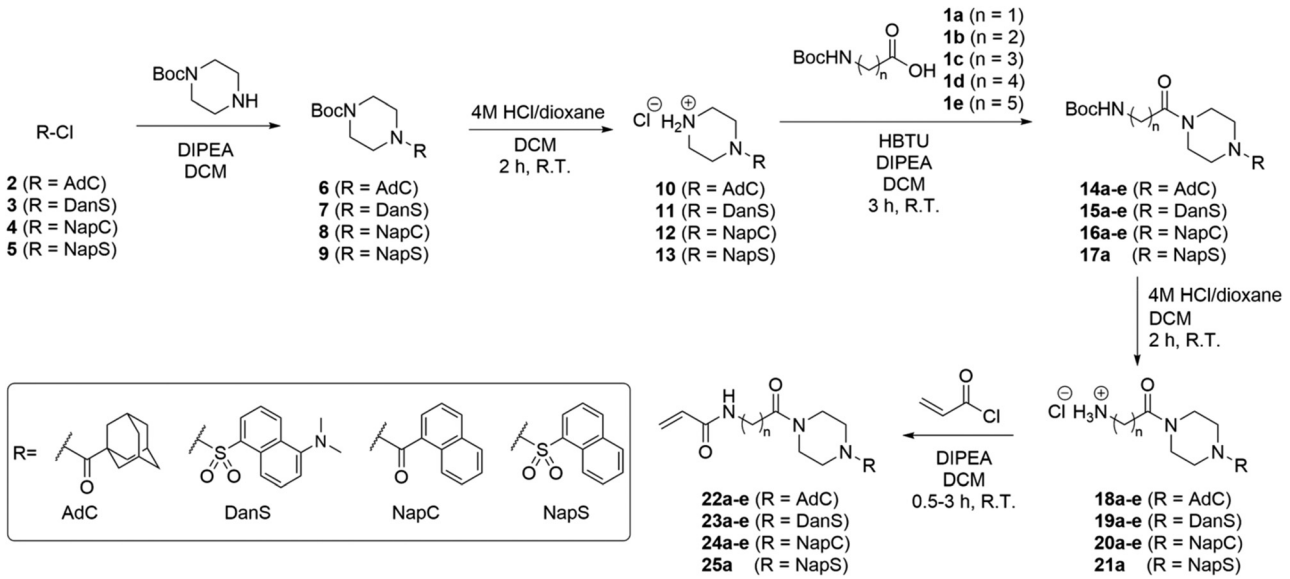

Scheme 1 Synthesis of inhibitors **22–25**. Abbreviations AdC, DanS, NapC, and NapS refer to hydrophobic moieties, adamantanecarbonyl, dansyl, naphthalenecarbonyl, and naphthalenesulfonyl, respectively. In all cases, a, b, c, d, and e refer to 1, 2, 3, 4, and 5 methylene units denoted $()_n$, respectively.

Boc deprotections using trifluoroacetic acid, we found this gave sticky solids with overall lower purity by TLC analysis. Conversely, the use of HCl in dioxane provided the amine HCl salts (**10–13**) as free-flowing powders following precipitation using DCM or Et_2O.

We initially planned to install the acryloyl group on the Ω-amino acids prior to coupling with the piperazine, but discovered that the acryloyl coupling reaction proceeded inefficiently, and the products were difficult to isolate. Therefore, we prepared Boc-protected amino acids **1a–e**, which, despite the addition of steps to the overall synthetic route, improved the yield, efficiency, and ease of synthesis at each step.

The coupling of functionalized piperazines **10–13** and Boc-protected amino acids **1a–e** was mediated by HBTU/DIPEA, which enabled rapid and clean conversion to the corresponding amides. We determined that the amides could be isolated by extraction through successive washes with dilute acid, brine, and saturated aqueous sodium bicarbonate. Following extraction, all amides **15–18** were pure by ^{1}H NMR except for compounds **15a** and **15b**, which required further purification by chromatography.

The subsequent Boc deprotection reactions were also performed using HCl/dioxane, which variably gave **18–21** as fine powders or foams, depending on linker chain length and hydrophobic unit. Coupling of the amines with acryloyl chloride gave the final inhibitor compounds, **22–25**. The first series of compounds to be synthesized was the naphthoyl series, which was purified at the final step by column chromatography. However, we later determined that the majority of compounds **23–25** could be obtained in >96% purity (as determined by HPLC analysis, see ESI†) simply following extraction and/or successive precipitation/washes with diethyl ether. This suggests that the naphthoyl series compounds (**24a–e**) could also have been purified in this way.

Kinetic evaluation

The series of inhibitors prepared herein were evaluated for their inhibition of recombinant human TG2 using an established kinetic assay.[26] The acyl transferase activity of TG2 was determined by monitoring the release of *p*-nitrophenolate product from the chromogenic substrate AL5.[36] Incubation with inhibitor resulted in the time-dependent loss of this activity, due to irreversible inhibition. The curves of absorbance *versus* time were fitted accordingly to a mono-exponential association equation, providing first order rate constants of inhibition, k_{obs} (Fig. 2A). These rate constants, measured at varied concentrations of inhibitor, were then fitted to a hyperbolic equation consistent with saturation kinetics, providing the inhibition parameters k_{inact} and K_I (Fig. 2B).

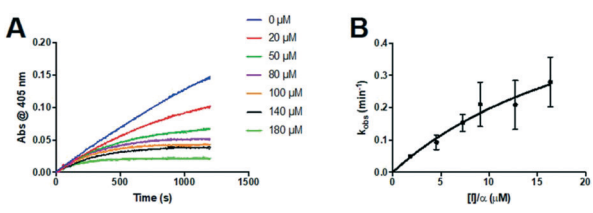

Fig. 2 Kinetic curves obtained during the inhibition of human TG2 with representative inhibitor **24a**. A) Observed rate constants (k_{obs}) for the loss of activity and B) hyperbolic fitting of the observed rate constants *versus* inhibitor concentration to a saturation kinetics model (see Materials and methods section).

Table 1 Inhibition parameters measured for the naphthoyl series of inhibitors, **24**

Cmpd.	n (CH_2)	k_{inact} (min^{-1})	K_I (μM)	k_{inact}/K_I (10^3 M^{-1} min^{-1})
24a	1	0.69 ± 0.26	25.0 ± 13.9	27.5 ± 18.6
24b	2	0.13 ± 0.02	51.6 ± 19.2	2.4 ± 1.0
24c	3	0.45 ± 0.06	134.0 ± 25.8	3.3 ± 0.8
24d	4	0.44 ± 0.08	141.9 ± 37.4	3.1 ± 1.0
24e	5	0.46 ± 0.15	109.3 ± 55.5	4.2 ± 2.6

The first series of inhibitors tested contained a naphthoyl hydrophobic group and a linker of varying length to which the pendant acrylamide warhead was tethered (Table 1). We were surprised to note that the shortest chain provided the most potent inhibition of TG2. We expected that inhibitors bearing the longest linkers would show the greatest affinity since we had observed this trend among many series of peptidomimetic TG2 inhibitors.[22,26,27,38] However, it is clear from the data shown in Table 1 that the shortest linker apparently positions the reactive acrylamide at the optimal distance from the active site cysteine, providing an efficiency (k_{inact}/K_I ratio) for compound **24a** of 27 500 M^{-1} min^{-1}, whereas the longer chain derivatives **24b–e** were roughly an order of magnitude less efficient.

In order to interrogate the effect of a different hydrophobic unit on the inhibition profile, the adamantyl series was also tested. Again, it was noted that the inhibitor having the shortest linker in the series (**22a**) also manifested the most potent inhibition, with a K_I value of 3.2 μM (Table 2). The efficiency of compound **22a**, as shown by its k_{inact}/K_I ratio, was also over an order of magnitude greater than that of naphthoyl derivative **24a**, indicating substantial preference for the adamantyl moiety. Compound **22a** is also known as EB-2-16,[34] and as compound **3e** in the study by Badarau *et al.*;[21] however, in that publication, its k_{inact}/K_I ratio was reported to be 171 875 M^{-1} min^{-1}, whereas in this study we measured a value of 412 × 10^3 M^{-1} min^{-1}. This difference may be due to the two different assays employed. While we used a direct chromogenic assay in this study, Badarau *et al.* used an indirect coupled-enzyme assay to measure k_{inact} and K_I.[39] It is possible that the initial lag period that is common to coupled enzyme assays may mask the initial phase of the inhibition reaction and under-report the rate constants of inactivation. This would result in slightly lower kinetic parameters than those measured herein by a direct chromogenic assay, which is more responsive over the initial time period of inhibition.

The dansyl series was the third library to be screened for TG2 inhibition. Increasing linker length again led to greatly diminished potency, with compound **23a** having the shortest linker and showing the highest potency (Table 3). It is important to note that **23a** was also first developed by the Griffin group. Compound **23a** is also known as EB-1-155,[34] or compound **3h** in the publication by Badarau *et al.*[21] Comparison of their k_{inact}/K_I value of 297 692 M^{-1} min^{-1}, to the value of 1508 × 10^3 M^{-1} min^{-1} measured herein, suggests that the coupled-enzyme assay again provided lower values than the direct chromogenic assay.

Finally, we evaluated one additional inhibitor that allowed two relevant structural comparisons. Inhibitor **25a** bears a naphthalenesulfonyl group in the place of the naphthoyl group of **24a**, while lacking only the dimethylamino group of **23a**. We hoped that the larger sulfonyl linkage would allow the naphthoyl group to bind deeper in the hydrophobic pocket of TG2, while allowing the piperazine–glycine linker to position the acrylamide warhead effectively. As shown in Table 4, inhibitor **25a** did show enhanced affinity relative to its carbonyl analogue **24a**, with the sulfonyl linkage decreasing the K_I value to 6.5 μM, while maintaining a k_{inact} of 0.70 min^{-1}, resulting in a k_{inact}/K_I ratio of 108 × 10^3 M^{-1} min^{-1}. Interestingly, the dimethylamino group of **23a** appears to substantially contribute to binding affinity, with its roughly 15-fold greater efficiency compared to **25a** being due to both its higher k_{inact} value and its lower K_I value.

Inspection of the kinetic parameters reported for the most potent inhibitors (*i.e.* **22a**, **23a** and **25a**) reveals significant standard error, deriving from the error of the hyperbolic fitting. In the Kitz & Wilson kinetic experiment used herein, as inhibitors become more efficient, they inactivate the enzyme very quickly, resulting in shorter reaction times and smaller end point absorbances (see Fig. 2A). This increases the error in the fitting of k_{obs}. Further, as k_{inact} increases for better inhibitors, it becomes increasingly difficult to measure k_{obs} values that approach k_{inact} (at saturation, see Fig. 2B), leading to error in the separate fitting of both K_I and k_{inact}. These errors are then propagated, leading to even greater relative error in the k_{inact}/K_I ratio. Therefore, we also performed simple linear regression on the k_{obs} values measured at the lowest concentrations of each inhibitor, allowing us to estimate the value of the k_{inact}/K_I ratio without

Table 2 Inhibition parameters of the adamantanecarbonyl series, **22**

Cmpd.	n (CH_2)	k_{inact} (min^{-1})	K_I (μM)	k_{inact}/K_I (10^3 M^{-1} min^{-1})
22a	1	1.34 ± 0.22	3.2 ± 1.0	412 ± 142
22b	2	n.d.	n.d.	n.d.
22c	3	n.d.	n.d.	n.d.
22d	4	0.19 ± 0.01	4.5 ± 1.2	41.9 ± 11.5
22e	5	0.36 ± 0.08	38.0 ± 15.4	9.5 ± 4.5

n.d.: no inhibition detected up to 100 μM.

Table 3 Inhibition parameters of the dansyl series, **23**

Cmpd.	n (CH_2)	k_{inact} (min^{-1})	K_I (μM)	k_{inact}/K_I (10^3 M^{-1} min^{-1})
23a	1	2.25 ± 1.44	1.49 ± 1.27	1508 ± 1608
23b	2	0.25 ± 0.02	64.5 ± 12.7	3.9 ± 0.9
23c	3	0.54 ± 0.31[a]	74.2 ± 42.9[a]	7.3 ± 0.5[a]
23d	4	0.55 ± 0.33	42.0 ± 4.3	13.1 ± 1.6
23e	5	0.23 ± 0.01	27.4 ± 1.6	8.6 ± 0.6

[a] Values obtained using double reciprocal fitting.

introducing as much error from fitting of the separate parameters. These ratios, reported for the best inhibitors of each series (**22a**, **23a**, **24a** and **25a**) in Table S1 in the ESI,† are all within experimental error of the ratios determined by hyperbolic fitting (Table 1–4), which lends confidence to the data treatment.

GTP binding evaluation

GTP binding is critical to the G-protein function of TG2, which has been implicated in a number of disease states.[40–42] However, it was not obvious to us that a small molecule inhibitor would be capable of preventing TG2 from adopting its closed conformation, forming its GTP binding site, and binding GTP.[17] Therefore, we decided to investigate whether our most efficient small molecule inhibitors, namely **22a**, **23a**, **24a** and **25a**, were indeed capable of blocking this activity. The results are presented in Fig. 3, as a fraction of the positive control, which represents maximum GTP binding to TG2, along with the blank (no TG2) representing zero GTP binding.

It is evident from Fig. 3 that all of the inhibitors tested are capable of inhibiting GTP binding, at least partially. To the best of our knowledge, this is the first explicit demonstration of the inhibition of GTP binding by these compounds, including those published previously (**22a** and **23a**).[21,34] It is interesting to note that these results appear to be aligned with those from another recent investigation,[20] in which we showed that sulforaphane, a very small irreversible inhibitor of TG2, is also able to partially inhibit GTP binding. Further studies are underway to determine the minimum steric bulk that is required to alter the conformational equilibrium of TG2 to completely abolish GTP binding.

Molecular docking analysis

As mentioned above, we were surprised to find that inhibitors bearing a shorter alkyl chain proved to be the most efficient of each series, since this is the opposite trend of what we have observed in series of peptidomimetic inhibitors. In an attempt to explain these unexpected results, we performed extensive molecular modelling studies, hoping to elucidate a functional binding model. Molecular Operating Environment (MOE) was therefore used to perform docking analysis on all inhibitors shown above. The computational binding affinities were prioritized based on a numerical value called the *S*-score, which decreases with improved predicted binding affinity.[43,44] Regarding the target protein, we used the structure of TG2 after reaction with a peptidic irreversible inhibitor (PDB code 2Q3Z), shown in Fig. 4.[16] The structure was prepared using the preparation tool from MOE. Water molecules, salts and ions were removed from the structure and all hydrogen atoms were displayed. The structure was verified, and corrected manually, for any problems or warnings such as chain breaks, termini missing or unreasonable charges. Two tryptophan residues, namely TRP241 and TRP332, form a tunnel leading to the active site nucleophilic residue CYS277 (orange) that is alkylated upon reaction with an acrylamide. These three residues are displayed in magenta. Moreover, six residues create the hydrophobic cavity targeted by our inhibitors, namely ALA304, LEU312, ILE313, PHE316, ILE331 and ILE421, all displayed in blue.

Each ligand was docked according to both a non-covalent and a covalent approach, using a rigid-body method that is

Table 4 Inhibition parameters of naphthalenesulfonyl inhibitor **25a**, relative to naphthoyl analogue **24a** and dansyl analogue **23a**

Cmpd.	n (CH_2)	k_{inact} (min^{-1})	K_I (μM)	k_{inact}/K_I (10^3 M^{-1} min^{-1})
23a	1	2.25 ± 1.44	1.49 ± 1.27	1508 ± 1608
24a	1	0.69 ± 0.26	25.0 ± 13.9	27.5 ± 18.6
25a	1	0.70 ± 0.13	6.51 ± 1.90	108 ± 38

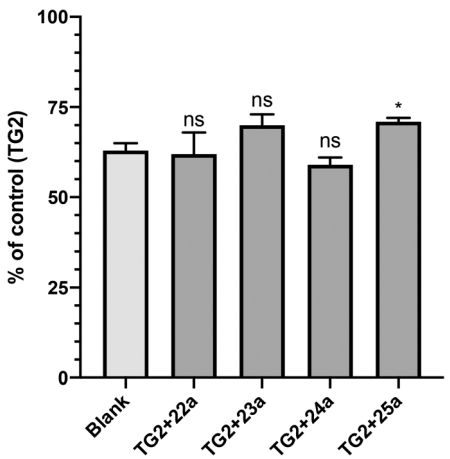

Fig. 3 GTP binding was measured using a fluorescent binding assay as described in the Materials and methods section. Inhibition of GTP binding was observed for all of the most efficient small molecule inhibitors studied herein (ns = not significant; *p value < 0.05, relative to blank).

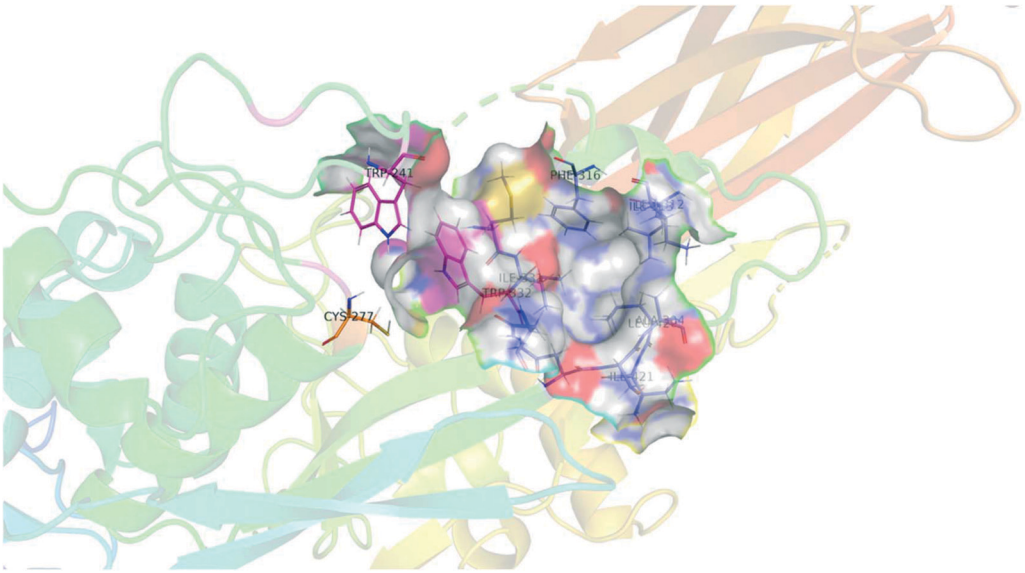

Fig. 4 Structural representation of TG2 binding site (PDB: 2Q3Z) in magenta, tryptophan residues TRP241 and TRP332 form a tunnel leading to the active site nucleophilic residue CYS277 (orange). Six residues create the hydrophobic cavity, namely ALA304, LEU312, ILE313, PHE316, MET330, ILE 331 and ILE421, all displayed in blue.

considered superior for covalent complexes.[44,45] The non-covalent approach involves calculation of *S* score values, prior to covalent bonding between the ligand and the receptor. Subsequently, the covalent bond is manually created between residue CYS277 and the acrylamide warhead of the bound inhibitor, followed by minimization of the system, which allows the ligand to adopt its final conformation. Alternatively, the covalent approach involves calculation of the potential binding affinities with the requirement of *in silico* covalent bond formation between CYS277 and the acrylamide warhead. To evaluate both sets of docking results, the *S* score values and the extent of insertion of each hydrophobic moiety into the hydrophobic cavity were considered. For the latter, the distances (*d*) between the centroids of the hydrophobic pocket and each hydrophobic structural moiety were measured. All results are presented in Table 5.

Table 5 Summary of docking results for inhibitors **22–24**

Hydrophobic moiety	Cmpd.	*n* CH_2	Non-covalent approach		Covalent approach	
			S score	*d* (Å)	*S* score	*d* (Å)
Adamantanecarbonyl	**22a**	1	−5.97	6.5	−5.12	6.5
	22b	2	−5.96	6.8	−5.28	6.5
	22c	3	−6.12	5.4	−5.72	6.1
	22d	4	−6.05	5.5	−5.86	4.5
	22e	5	−6.81	5.5	−6.00	5.9
Dansyl	**23a**	1	−5.40	7.8	−4.86	6.1
	23b	2	−6.78	4.9	−5.71	5.5
	23c	3	−6.49	6.7	−5.41	8.6
	23d	4	−6.48	4.5	−5.41	5.9
	23e	5	−6.97	3.5	−6.53	6.8
Naphthoyl	**24a**	1	−6.24	7.0	−5.77	5.0
	24b	2	−6.28	4.7	−6.00	4.9
	24c	3	−6.90	5.0	−5.82	4.7
	24d	4	−6.92	4.7	−6.05	4.2
	24e	5	−7.30	4.6	−6.41	4.6

As we originally expected, docking of the longer chain derivatives provided better potential binding affinity as well as deeper insertion into the hydrophobic cavity. For each series of hydrophobic moiety, the inhibitor comprising a 5-carbon tether displays the best *S* score value compared to the inhibitors bearing a spacer of only 1 carbon. The same trend is observed for the insertion depth of each hydrophobic moiety in the hydrophobic cavity of TG2. Understandably, inhibitors with longer chains tend to show deeper insertion, hence improved hydrophobic interactions with the enzyme. Furthermore, the dansyl **23(a–e)** and the naphthoyl **24(a–e)** series were predicted to bind more deeply than the adamantyl series **22(a–e)**, based on the average insertion distances of 5.4, 5.2 and 5.9 Å, respectively. Representations of the inhibitors predicted to show the weakest and strongest affinity for each series are shown in Fig. 5. In summary, the binding models predicted by docking, and the experimental data obtained through kinetic studies are inconsistent with each other. For example, molecular modelling predicts that the inhibitor with the longest tether to acrylamide on one end, and a naphthoyl group on the other (*i.e.* **24e**) should be the best inhibitor, when in reality, **24e** is one of the least efficient tested herein.

In contrast, the inhibitor bearing a dansyl group and the shortest tether (*i.e.* **23a**, aka EB-1-155) was predicted by molecular modelling to have the lowest affinity, but in reality it is the best tested herein, and indeed one of the most efficient inhibitors known for TG2.[26] In light of this, we repeated our docking simulations, using a different structure deposited in the PDB. Structure 3S3J was obtained after inhibition of TG2 with a peptidic irreversible inhibitor (Cbz-

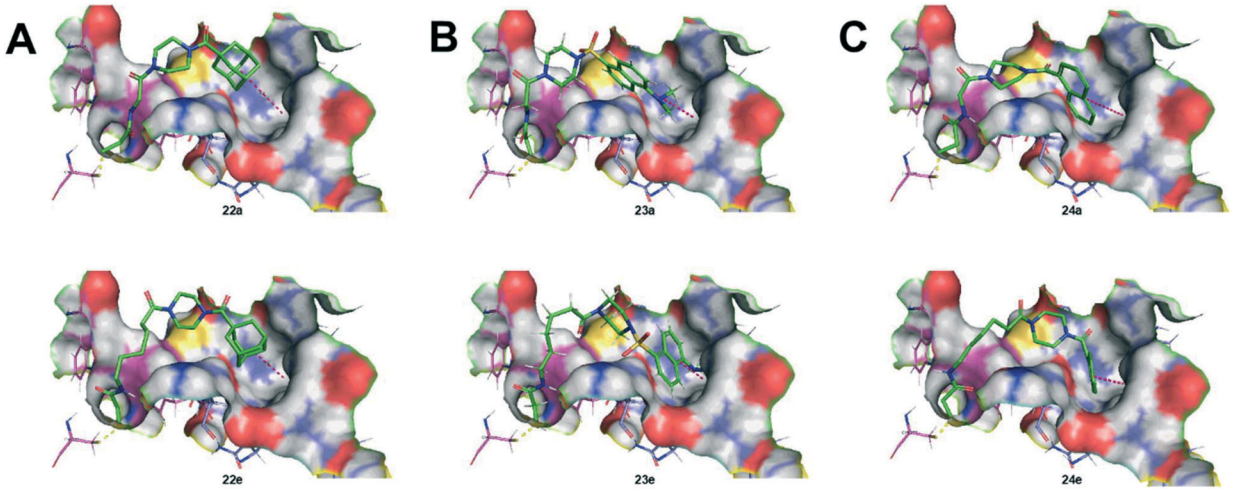

Fig. 5 Structural representation of the inhibitors of each series predicted to show the weakest and strongest affinity, based on molecular docking *via* the non-covalent approach. A) Inhibitors **22a** (upper) and **22e** (lower); B) inhibitors **23a** (upper) and **23e** (lower); C) inhibitors **24a** (upper) and **24e** (lower).

DON-Val-Pro-Leu-OH) that is different than the one used to generate 2Q3Z (Ac-Pro-DON-Leu-Pro-Phe-NH_2). That being said, the substrate binding sites of both crystallographic structures are very similar (see Fig. S1, ESI†). Unsurprisingly, the docking simulations performed with 3S3J provided the same trend in *S* scores as in 2Q3Z, again in opposition to our observed kinetic results (see Table S2, ESI†).

The discrepancy between the molecular modelling predictions and the experimental evidence obtained by kinetic studies leads us to question whether these crystallographic structures are appropriate for the docking of our small molecule inhibitors. Although 2Q3Z and 3S3J are the most relevant crystallographic structures deposited in the PDB, it is important to note that they were both obtained after inhibition with peptidic inhibitors, whose C-terminal residues may define the very shape of the hydrophobic pocket 'D-site'. However, in the absence of inhibitor, any enzyme may adopt a conformation that differs from its crystallographic structure, and this may be especially true for TG2, an enzyme known to undergo dramatic and dynamic conformational changes.[16,46,47] The free enzyme may simply adopt a conformation sufficiently different from that of the crystallographic structure, that precludes the use of that structure to predict how small molecule inhibitors may bind to the enzyme. This underlines the pressing need for additional protein crystallography studies with small molecule inhibitors. But in the absence of such structures, rigorous kinetic data from SAR studies will be critical for the design of future inhibitors.

Materials and methods

Synthesis

General remarks. All reagents and solvents were purchased from commercial sources and used without further purification. ^{1}H and ^{13}C NMR spectra were recorded on a Bruker 400 MHz spectrometer, and chemical shifts were reported in ppm referenced to the deuterated solvent peak. High resolution mass spectra were obtained with a quadrupole time-of-flight (QTOF) analyzer and electrospray ionization (ESI). Thin-layer chromatography (TLC) was performed using aluminium-backed silica plates and visualized using UV light, unless otherwise specified. Plates were eluted using TLC solvent system 1 (10% MeOH, 45% DCM, and 45% hexanes) or TLC solvent system 2 (10% MeOH, 44.5% DCM, 44.5% hexanes, and 1% triethylamine), or else as specified.

General procedure for the synthesis of compounds 1a–e (GP1). Amino acid (3.367 mmol) was stirred in 1 M NaOH (12 mL) and dioxane (6 mL) at 0 °C for 10 min. Boc anhydride (1102 mg, 5.051 mmol) was added, and the reaction mixture was stirred overnight. When complete by TLC analysis (10% MeOH in DCM, stained with ninhydrin), the reaction mixture was concentrated *in vacuo* until the dioxane was removed, then the solution was extracted with Et_2O. The aqueous phase was acidified through dropwise addition of 12 M HCl, and then extracted with EtOAc (2 × 15 mL). The organic phase was dried with $MgSO_4$, filtered, and the filtrate evaporated *in vacuo* to give a clear oil, which dried to a white crystalline solid.

***N*-[(1,1-Dimethylethoxy)carbonyl]glycine (1a).** Following **GP1**, recovered 520 mg/88% of product.

***N*-[(1,1-Dimethylethoxy)carbonyl]-β-alanine (1b).** Following **GP1**, recovered 545 mg/86% of product.

***N*-[(1,1-Dimethylethoxy)carbonyl]-4-aminobutyric acid (1c).** Following **GP1**, recovered 645 mg/94% of product.

***N*-[(1,1-Dimethylethoxy)carbonyl]-5-aminovaleric acid (1d).** Following **GP1**, recovered 478 mg/65% of product.

***N*-[(1,1-Dimethylethoxy)carbonyl]-6-aminocaproic acid (1e).** Following **GP1**, recovered 739 mg/95% of product.

Adamantanecarbonyl chloride (2). To a stirred solution of adamantane-1-carboxylic acid (700 mg, 3.884 mmol) in DCM

(3 mL) was added thionyl chloride (1 mL). The reaction was monitored by ^{1}H NMR analysis and was complete after 2 h. The reaction was evaporated to dryness under reduced pressure, and co-evaporated with a small amount of DCM, to give the product as a white, crystalline solid (752 mg, >95%) which was carried forward without further purification.

General procedure for the synthesis of compounds 6–9 (GP2). *N*-Boc-piperazine (1.1 equiv.) and DIPEA (2 equiv.) were stirred in DCM (0.25 M) at R.T. To the stirring solution was added **2–5** (1 equiv.). The reaction was complete by TLC analysis (1 : 1 hexanes : ethyl acetate) after 10 min. The reaction mixture was diluted in DCM (10 mL) and washed with 5% AcOH (2 × 10 mL) and brine (2 × 10 mL). The organic phase was dried with $MgSO_4$ and solvent removed under reduced pressure.

***N*-(Adamantanecarbonyl)-*N*′-Boc-piperazine (6).** Following **GP2**, from 400 mg (2.013 mmol) of **2**, collected 640 mg of **6** as a white solid (>95%). ^{1}H NMR (400 MHz, $CDCl_3$) δ 3.65 (t, J = 4.8 Hz, 1H), 3.40 (q, J = 3.5 Hz, 1H), 2.04 (s, 1H), 1.98 (d, J = 2.8 Hz, 1H), 1.72 (d, J = 2.2 Hz, 1H), 1.46 (s, 1H).

***N*-Dansyl-*N*′-boc-piperazine (7).** Compound **7** was prepared following a reported procedure. Characterization data are consistent with literature.[48]

***N*-(Naphthalenecarbonyl)-*N*′-boc-piperazine (8).** Following **GP2**, from 1861 mg (0.762 mmol) of **4**, collected 3052 mg of **8** as a white solid (92%). Characterization data are consistent with literature.[26]

***N*-(Naphthalenesulfonyl)-*N*′-boc-piperazine (9).** Following **GP2**, from 300 mg (0.1324 mmol) of **5**, collected 453 mg of **9** as a white solid (91%). Characterization data are consistent with literature.[49]

General procedure for the synthesis of compounds 10–13 (GP3). Compound **6–9** was stirred in a 1 : 1 v/v solution of DCM and HCl (4 M in dioxane) at an overall concentration of ~0.25 M. The reaction proceeded until starting material was consumed as determined by TLC analysis (solvent system 1) (approximately 2 h). The reaction mixture was evaporated *in vacuo* and coevaporated with DCM. The resulting residue was triturated with Et_2O, which was decanted off to give the product as a powdery solid. The HCl salts recovered were carried forward without further purification.

***N*-(Adamantanecarbonyl)piperazine hydrochloride (10).** Following **GP3**, from 600 mg (1.724 mmol) of **6**, recovered 408 mg of **10** as a free-flowing white solid.

***N*,*N*-Dimethyl-5-(1-piperazinylsulfonyl)-1-naphthalenamine hydrochloride (11).** Following **GP3**, from 1.63 g (3.89 mmol) of **7**, recovered 1.35 g of **11** as an off-white solid.

***N*-(Naphthalenecarbonyl)piperazine hydrochloride (12).** Following **GP3**, from 1500 mg (4.406 mmol) of **8**, recovered 860 mg of **12** as a powdery white solid.

***N*-(Naphthalenesulfonyl)piperazine hydrochloride (13).** Following **GP3**, from 400 mg (1.063 mmol) of **9**, recovered 231 mg of **13** as a white solid.

General procedure for the synthesis of compounds 14a–e (GP4). Boc-protected amino acids **1a–e** (0.463 mmol), HBTU (255 mg, 0.674 mmol), and DIPEA (294 μL, 1.684 mmol) were stirred in DCM (6 mL) at R.T. After 1 h, compound **10** (120 mg, 0.421 mmol) was added. Upon completion by TLC analysis (1 : 1 hexanes : ethyl acetate, stained with ninhydrin), the solvent was evaporated *in vacuo*, then the reaction mixture was redissolved in EtOAc (~20 mL). The organic phase was washed with 5% AcOH (3 × 10 mL), brine (20 mL), $NaHCO_3$ (20 mL) and brine again (20 mL). The organic phase was dried over $MgSO_4$ and evaporated. The resulting product was washed with Et_2O or pentane as needed.

***N*-2-[4-[[1-Adamantanecarbonyl]-1-piperazinyl]-2-oxoethyl] carbamic acid *tert*-butyl ester (14a).** Following **GP4**, the product was collected as a white solid following Et_2O wash (126 mg, 74%). ^{1}H NMR (400 MHz, $CDCl_3$) δ 5.47 (br. s, 1H), 3.96 (d, J = 4.3 Hz, 2H), 3.69 (m, 4H), 3.61 (m, 2H), 3.38 (m, 1H), 2.05 (br. s, 3H), 1.97 (m, 6H), 1.72 (m, 6H, overlaps with H_2O resonance), 1.44 (s, 9H). ^{13}C NMR (101 MHz, $CDCl_3$) δ 176.10, 167.26, 155.81, 79.82, 45.27, 44.70, 44.49, 42.25, 42.18, 41.78, 39.07, 36.54, 28.37, 28.35. HRMS (ESI) calc'd for $C_{22}H_{35}N_3O_4Na$ ([MNa]$^+$): 428.2525, found: 428.2536.

***N*-3-[4-[[1-Adamantanecarbonyl]-1-piperazinyl]-3-oxopropyl] carbamic acid *tert*-butyl ester (14b).** Following **GP4**, the product was collected as a white solid following pentane wash (172 mg, >95%). ^{1}H NMR (400 MHz, $CDCl_3$) δ 5.25 (br. s, 1H), 3.68 (m, J = 3.3 Hz, 4H), 3.59 (m, 2H), 3.42 (m, 4H), 2.52 (t, J = 5.7 Hz, 2H), 2.05 (s, 3H), 1.98 (m, 6H), 1.72 (m, 6H, overlaps with H_2O resonance), 1.42 (s, 9H). ^{13}C NMR (101 MHz, $CDCl_3$) δ 176.22, 170.52, 156.15, 79.37, 45.49, 45.00, 41.89, 41.85, 39.19, 36.68, 36.34, 33.55, 28.55, 28.51. HRMS (ESI) calc'd for $C_{23}H_{37}N_3O_4Na$ ([MNa]$^+$): 442.2682, found: 442.2681.

***N*-4-[4-[[1-Adamantanecarbonyl]-1-piperazinyl]-4-oxobutyl] carbamic acid *tert*-butyl ester (14c).** Following **GP4**, the product was collected as a white solid following pentane wash (113 mg, 62%). ^{1}H NMR (400 MHz, $CDCl_3$) δ 4.75 (br. s, 1H), 3.68 (m, 4H), 3.60 (m, 2H), 3.44 (m, 2H), 3.18 (q, J = 5.8 Hz, 2H), 2.37 (t, J = 7.2 Hz, 2H), 2.05 (s, 3H), 1.98 (m, 6H), 1.84 (qu, J = 6.9 Hz, 2H), 1.71 (m, 6H, overlaps with H_2O resonance), 1.43 (s, 9H). ^{13}C NMR (101 MHz, $CDCl_3$) δ 176.10, 171.27, 156.12, 79.27, 45.59, 45.50, 44.88, 41.86, 41.77, 39.07, 36.57, 30.48, 28.42, 28.40, 25.38. HRMS (ESI) calc'd for $C_{24}H_{39}N_3O_4Na$ ([MNa]$^+$): 456.2838, found: 456.2836.

***N*-5-[4-[[1-Adamantanecarbonyl]-1-piperazinyl]-5-oxopentyl] carbamic acid *tert*-butyl ester (14d).** Following **GP4**, the product was collected as a white solid following Et_2O wash (164 mg, 87%). ^{1}H NMR (400 MHz, $CDCl_3$) δ 4.55 (br. s, 1H), 3.68 (m, 4H), 3.60 (m, 2H), 3.45 (m, 2H), 3.11 (m, 2H), 2.33 (t, J = 7.5 Hz, 2H), 2.05 (s, 3H), 1.98 (m, 6H), 1.74 (m, 6H, overlaps with H_2O resonance), 1.65 (m, 2H), 1.50 (m, 2H), 1.43 (s, 9H), 1.37 (m, 2H). ^{13}C NMR (101 MHz, $CDCl_3$) δ 176.23, 156.18, 79.39, 45.72, 45.06, 41.90, 40.20, 39.20, 36.70, 32.78, 29.85, 28.56, 28.54, 22.27. HRMS (ESI) calc'd for $C_{25}H_{41}N_3O_4Na$ ([MNa]$^+$): 470.2995, found: 470.2975.

***N*-6-[4-[[1-Adamantanecarbonyl]-1-piperazinyl]-6-oxohexyl] carbamic acid *tert*-butyl ester (14e).** Following **GP4**, the product was collected as a white solid following a wash with 1 : 1 pentane : Et_2O (140 mg, 72%). ^{1}H NMR (400 MHz, $CDCl_3$)

δ 4.62 (br. s, 1H), 3.67 (m, 4H), 3.60 (m, 2H), 3.45 (m, 2H), 3.13 (m, 2H), 2.36 (t, J = 7.4 Hz, 2H), 2.05 (s, 3H), 1.99 (m, 6H), 1.71 (m, 6H, overlaps with H_2O resonance), 1.62 (app. s, 4H), 1.53 (m, 2H), 1.43 (s, 9H). ^{13}C NMR (101 MHz, $CDCl_3$) δ 176.23, 156.18, 79.39, 45.72, 45.06, 41.90, 40.20, 39.20, 36.70, 32.78, 29.85, 28.56, 28.54, 22.27. HRMS (ESI) calc'd for $C_{26}H_{43}N_3O_4Na$ ($[MNa]^+$): 484.3151, found: 484.3148.

***N*-2-[4-[[5-(Dimethylamino)-1-naphthalenyl]sulfonyl]-1-piperazinyl]-2-oxoethylcarbamic acid *tert*-butyl ester (15a).** Compound **1a** (0.308 g, 1.76 mmol) was dissolved in DCM (8 mL). HBTU (0.6432 g, 1.70 mmol) and DIPEA (330 μL, 1.89 mmol) was added and left to stir for 1 h. Compound **3** (300 mg, 0.842 mmol) was added, and the solution was left to stir overnight. Reaction was confirmed to be complete *via* TLC (solvent system 1) and solvent was removed *in vacuo*. The residue was redissolved in 10 mL of ethyl acetate, and washed with 10% acetic acid, brine, and bicarbonate (2 × 10 mL each). The organic phase was dried with $MgSO_4$, and the solvent was removed *in vacuo*. The product was purified using flash chromatography (solvent system 2) and appeared as a yellow residue (249 mg, 62%). Characterization data are consistent with literature.[21]

***N*-3-[4-[[5-(Dimethylamino)-1-naphthalenyl]sulfonyl]-1-piperazinyl]-3-oxopropylcarbamic acid *tert*-butyl ester (15b).** Compound **1b** (0.280 g, 1.48 mmol) was dissolved in DCM (8 mL). HBTU (0.8369 g, 2.21 mmol) and DIPEA (940 μL, 5.40 mmol) was added and left to stir for 1 h. Compound **3** (303 mg, 0.850 mmol) was added, and the solution was left to stir overnight. The reaction was confirmed to be complete *via* TLC (solvent system 1) and solvent was removed *in vacuo*. The reaction mixture was redissolved in 10 mL of ethyl acetate, and washed 10% acetic acid, brine, and bicarbonate (2 × 10 mL each). The organic phase was dried with $MgSO_4$, and the solvent was removed *in vacuo*. The product was purified using flash chromatography (solvent system 2) and appeared as a yellow residue (329 mg, 79%). ^{1}H NMR (400 MHz, $CDCl_3$) δ 8.50 (d, J = 8.5 Hz, 1H), 8.28 (d, J = 8.7 Hz, 1H), 8.11 (d, J = 7.2 Hz, 1H), 7.46 (t, J = 8.0 Hz, 2H), 7.10 (d, J = 7.5 Hz, 1H), 3.54 (t, J = 4.8 Hz, 2H), 3.38 (m, 2H), 3.24 (q, J = 5.6 Hz, 2H), 3.10 (m, 4H), 2.80 (s, 6H), 2.34 (t, J = 5.6 Hz, 2H), 1.29 (s, 9H). ^{13}C NMR (101 MHz, $CDCl_3$) δ 170.00, 155.93, 151.84, 132.20, 131.02, 130.70, 130.24, 130.03, 128.22, 123.13, 119.23, 115.33, 79.03, 53.46, 51.63, 45.53, 45.32, 44.84, 40.95, 28.30, 19.84. HRMS (ESI) calc'd for $C_{24}H_{34}N_4O_5SNa$ ($[MNa]^+$): 513.2148, found: 513.2121.

General procedure for the synthesis of compounds 15c–e (GP5). Boc-protected amino acid **1c–e** (0.422 mmol), HBTU (233 mg, 0.614 mmol) and DIPEA (267 μL, 1.536 mmol) were stirred in DCM (8 mL). After 1 h, compound **11** (150 mg, 0.384 mmol) was added. The reaction was complete by TLC analysis (10% MeOH in DCM) 2.5 h following the addition of **11**. The solvent was evaporated *in vacuo*, then the residue redissolved in EtOAc (20 mL) and washed with 5% AcOH (2 × 10 mL), brine (10 mL), saturated $NaHCO_3$ (3 × 10 mL) and brine again (10 mL). The organic phase was collected, dried over $MgSO_4$, and evaporated, then triturated with Et_2O and dried under vacuum to give the product as a light yellow solid.

***N*-4-[4-[[5-(Dimethylamino)-1-naphthalenyl]sulfonyl]-1-piperazinyl]-4-oxobutylcarbamic acid *tert*-butyl ester (15c).** Following **GP5**, collected 168 mg/87% of product. ^{1}H NMR (400 MHz, $CDCl_3$) δ 8.58 (d, J = 8.5 Hz, 1H), 8.37 (d, J = 8.7 Hz, 1H), 8.20 (dd, J = 1.2, 7.4 Hz, 1H), 7.54 (dd, J = 7.5, 8.6 Hz, 2H), 7.19 (d, J = 7.0 Hz, 1H), 4.67 (s, 1H), 3.64 (t, J = 5.1 Hz, 2H), 3.48 (t, J = 5.0 Hz, 2H), 3.17 (m, 4H), 3.10 (q, J = 6.5 Hz, 2H), 2.89 (s, 6H), 2.26 (t, J = 6.69 Hz, 2H), 1.74 (qu, J = 6.98 Hz, 2H), 1.39 (s, 9H). ^{13}C NMR (101 MHz, $CDCl_3$) δ 171.02, 156.20, 151.83, 132.39, 131.13, 130.94, 130.45, 130.17, 128.39, 123.37, 119.59, 115.55, 79.31, 45.76, 45.59, 45.21, 41.25, 40.19, 30.45, 28.51, 25.40. HRMS (ESI) calc'd for $C_{25}H_{36}N_4O_5SNa$ ($[MNa]^+$): 527.2304, found: 527.2322.

***N*-5-[4-[[5-(Dimethylamino)-1-naphthalenyl]sulfonyl]-1-piperazinyl]-5-oxopentylcarbamic acid *tert*-butyl ester (15d).** Following **GP5**, collected 187 mg/94% of product. ^{1}H NMR (400 MHz, $CDCl_3$) δ 8.58 (d, J = 8.5 Hz, 1H), 8.38 (d, J = 8.7 Hz, 1H), 8.20 (dd, J = 1.2, 7.3 Hz, 1H), 7.54 (dd, J = 7.5, 8.6 Hz, 2H), 7.20 (d, J = 7.4 Hz, 1H), 4.57 (br. s, 1H), 3.63 (t, J = 4.9 Hz, 2H), 3.49 (t, J = 4.9 Hz, 2H), 3.16 (m, 4H), 3.08 (q, J = 6.4 Hz, 2H), 2.89 (s, 6H), 2.25 (t, J = 7.4 Hz, 2H), 1.58 (qu, J = 6.0 Hz, 1H), 1.41 (m, several overlapping signals, 13H). ^{13}C NMR (101 MHz, $CDCl_3$) δ 171.26, 156.14, 151.76, 132.39, 131.12, 130.97, 130.47, 130.14, 128.37, 123.41, 119.68, 115.58, 79.27, 45.83, 45.61, 45.22, 41.19, 40.08, 32.60, 29.73, 28.53, 22.10. HRMS (ESI) calc'd for $C_{26}H_{38}N_4O_5SNa$ ($[MNa]^+$): 541.2461, found: 541.2466.

***N*-6-[4-[[5-(Dimethylamino)-1-naphthalenyl]sulfonyl]-1-piperazinyl]-6-oxohexylcarbamic acid *tert*-butyl ester (15e).** Following **GP5**, collected 198 mg/97% of product. ^{1}H NMR (400 MHz, $CDCl_3$) δ 8.58 (d, J = 8.5 Hz, 1H), 8.38 (d, J = 8.7 Hz, 1H), 8.20 (dd, J = 1.2, 7.4 Hz, 1H), 7.54 (dd, J = 7.5, 8.5 Hz, 2H), 7.19 (d, J = 7.2 Hz, 1H), 4.53 (s, 1H), 3.63 (t, J = 4.9 Hz, 2H), 3.48 (t, J = 4.9 Hz, 2H), 3.16 (m, 4H), 3.06 (q, J = 6.5 Hz, 2H), 2.89 (s, 6H), 2.22 (t, J = 7.5 Hz, 2H), 1.55 (qu, J = 7.6 Hz, 2H), 1.41 (s, several overlapping signals, 13H), 1.29 (m, 2H). ^{13}C NMR (101 MHz, $CDCl_3$) δ 171.41, 156.11, 151.80, 132.38, 131.09, 130.96, 130.47, 130.15, 128.37, 123.37, 119.62, 115.54, 79.20, 45.82, 45.59, 45.24, 41.15, 40.42, 33.09, 29.96, 28.54, 26.58, 24.72. HRMS (ESI) calc'd for $C_{27}H_{40}N_4O_5SNa$ ($[MNa]^+$): 555.2617, found: 555.2638.

General procedure for the synthesis of compounds 16a–e (GP6). Boc-protected amino acid **1a–e** (0.517 mmol), HBTU (285 mg, 0.752 mmol) and DIPEA (327 μL 1.880 mmol), were stirred in DCM (8 mL) at R.T. After 1 h, compound **12** (130 mg, 0.470 mmol) was added. The reaction was complete by TLC analysis (TLC solvent system 2) 1.5 h after addition of **12**, and a small amount of precipitate had formed. The reaction mixture was filtered, and the filtrate collected and concentrated *in vacuo*. The resulting residue was redissolved in EtOAc (20 mL) and washed with 10% AcOH (2 × 15 mL), sat. $NaHCO_3$ (2 × 15 mL) and brine (10 mL). The organic phase was collected, dried over $MgSO_4$, and evaporated to dryness. The residue was coevaporated with Et_2O to give a white foam.

***N*-2-[4-[[1-Naphthalenecarbonyl]-1-piperazinyl]-2-oxoethyl] carbamic acid *tert*-butyl ester (16a).** Following **GP6**, collected 157 mg/84% of product. ^{1}H NMR (400 MHz, $CDCl_3$) δ 7.90 (m, 2H), 7.80 (m, 1H), 7.51 (m, 3H), 7.42 (dd, J = 1.2, 7.0 Hz, 1H), 5.44 (s, 1H), 4.08-3.15 (m, 10H), 1.44 (2 overlapping singlets (rotamers), 9H). ^{13}C NMR (101 MHz, $CDCl_3$) δ 155.80, 133.53, 129.66, 129.51, 128.64, 127.31, 126.68, 125.19, 124.41, 123.97, 79.88, 46.75, 44.83, 44.37, 42.42, 41.92, 41.63, 28.34. HRMS (ESI) calc'd for $C_{22}H_{27}N_3O_4Na$ ([MNa]$^+$): 420.1899, found: 420.1905.

***N*-3-[4-[[1-Naphthalenecarbonyl]-1-piperazinyl]-3-oxopropyl] carbamic acid *tert*-butyl ester (16b).** Following **GP6**, collected 175 mg/91% of product. ^{1}H NMR (400 MHz, $CDCl_3$) δ 7.89 (m, 2H), 7.81 (m, 1H), 7.51 (m, 3H), 7.42 (dd, J = 1.2, 7.0 Hz, 1H), 5.20 (s, 1H), 3.16–4.07 (m, 10H), 2.58 (t, J = 5.5 Hz, 1H), 2.43 (br. s, 1H), 1.42 (2 overlapping singlets (rotamers), 1H). ^{13}C NMR (101 MHz, $CDCl_3$) δ 155.99, 133.52, 129.56, 128.62, 127.27, 126.65, 125.19, 124.44, 123.95, 79.32, 46.83, 45.74, 45.19, 41.97, 41.47, 36.28, 33.47, 28.42. HRMS (ESI) calc'd for $C_{23}H_{29}N_3O_4Na$ ([MNa]$^+$): 434.2056, found: 434.2068.

***N*-4-[4-[[1-Naphthalenecarbonyl]-1-piperazinyl]-4-oxobutyl] carbamic acid *tert*-butyl ester (16c).** Following **GP6**, collected 185 mg/92% of product. ^{1}H NMR (400 MHz, $CDCl_3$) δ 7.89 (m, 2), 7.81 (m, 1H), 7.51 (m, 3H), 7.41 (dd, J = 1.2, 7.0 Hz, 1H), 4.71 (s, 1H), 4.05–3.07 (m, 10H), 2.43 (t, J = 7.0 Hz, 1H), 2.29 (br. s, 1H), 1.83 (m, 2H), 1.42 (2 overlapping singlets (rotamers), 9H). ^{13}C NMR (101 MHz, $CDCl_3$) δ 156.13, 133.52, 129.57, 129.52, 128.60, 127.25, 126.63, 125.18, 124.47, 123.93, 79.30, 46.91, 45.95, 45.40, 41.89, 41.59, 40.23, 30.41, 28.42, 25.41. HRMS (ESI) calc'd for $C_{24}H_{31}N_3O_4Na$ ([MNa]$^+$): 448.2212, found: 448.2227.

***N*-5-[4-[[1-Naphthalenecarbonyl]-1-piperazinyl]-5-oxopentyl] carbamic acid *tert*-butyl ester (16d).** Following **GP6**, collected 142 mg/68% of product. ^{1}H NMR (400 MHz, $CDCl_3$) δ 7.89 (m, 2H), 7.81 (m, 1H), 7.51 (m, 3H), 7.42 (d, J = 6.9 Hz, 1H), 4.60 (s, 1H), 4.05–3.03 (m, 10H), 2.41 (t, J = 7.1 Hz, 1H), 2.26 (br. s, 1H), 1.66 (m, 2H), 1.57–1.31 (m, 2 overlapping signals, 11H). ^{13}C NMR (101 MHz, $CDCl_3$) δ 171.48, 156.04, 133.52, 129.53, 128.60, 127.24, 126.63, 125.18, 124.49, 123.93, 79.19, 47.25, 46.92, 45.38, 41.93, 41.70, 39.92, 32.62, 29.71, 28.42, 22.11. HRMS (ESI) calc'd for $C_{25}H_{33}N_3O_4Na$ ([MNa]$^+$): 462.2369, found: 462.2376.

***N*-6-[4-[[1-Naphthalenecarbonyl]-1-piperazinyl]-6-oxohexyl] carbamic acid *tert*-butyl ester (16e).** Following **GP6**, collected 213 mg/93% of product. ^{1}H NMR (400 MHz, $CDCl_3$) δ 7.89 (m, 2H), 7.81 (m, 1H), 7.51 (m, 3H), 7.42 (d, J = 6.8 Hz, 2H), 4.54 (s, 1H), 4.05–3.02 (m, 10H), 2.37 (t, J = 7.5 Hz, 1H), 2.24 (br. s, 1H), 1.64 (m, 1H), 1.56–1.23 (m, 3 overlapping signals, 13H). ^{13}C NMR (101 MHz, $CDCl_3$) δ 169.76, 156.01, 133.52, 129.54, 128.59, 127.24, 126.63, 125.19, 124.50, 123.94, 79.16 (determined by HMBC), 47.27, 46.94, 45.43, 41.97, 40.34, 33.10, 29.91, 28.43, 26.51, 24.73. HRMS (ESI) calc'd for $C_{26}H_{35}N_3O_4Na$ ([MNa]$^+$): 476.2525, found: 476.2538.

***N*-2-[4-[[1-Naphthalenesulfonyl]-1-piperazinyl]-2-oxoethyl] carbamic acid *tert*-butyl ester (17a).** Boc-glycine (74 mg, 0.422 mmol), HBTU (233 mg, 0.614 mmol), and DIPEA (267 μL, 1.536 mmol) were stirred in DCM (5 mL) at R.T. After 1 h, **13** (120 mg, 0.384 mmol) was added. The reaction was complete by TLC analysis 2.5 h following addition of **13**. The solvent was removed *in vacuo* and the residue redissolved in EtOAc (20 mL). The organic phase was washed with 5% aqueous acetic acid (3 × 10 mL), brine (20 mL), saturated aqueous $NaHCO_3$ (20 mL), and brine (10 mL). The organic phase was dried over $MgSO_4$ and evaporated to dryness. The resulting residue was washed with Et_2O and dried under vacuum to give the product as a white solid (161 mg, >95%). ^{1}H NMR (400 MHz, $CDCl_3$) δ 8.71 (d, J = 8.8 Hz, 1H), 8.21 (dd, J = 1.2, 7.4 Hz, 1H), 8.11 (d, J = 8.2 Hz, 1H), 7.95 (dd, J = 1.5, 8.0 Hz, 1H), 7.62 (m, 3H), 5.36 (s, 1H), 3.85 (d, J = 4.3 Hz, 2H), 3.66 (t, J = 5.1 Hz, 2H), 3.43 (t, J = 4.9 Hz, 2H), 3.18 (m, 4H), 1.40 (s, 9H). ^{13}C NMR (101 MHz, $CDCl_3$) δ 167.05, 155.84, 135.14, 134.55, 131.98, 130.99, 129.26, 128.97, 128.55, 127.23, 124.93, 124.32, 80.00, 45.61, 45.48, 44.17, 42.25, 41.61, 28.43. HRMS (ESI) calc'd for $C_{21}H_{27}N_3O_5SNa$ ([MNa]$^+$): 456.1569, found: 456.1552.

General procedure for the synthesis of compounds 18–21 (GP7). Compound **14–17** (1 equiv.) was dissolved in 1 : 1 DCM and HCl (4 M in dioxane) at an overall concentration of ~0.1 M. Disappearance of the starting material was monitored by thin layer chromatography (10% MeOH in DCM), and upon completion, the reaction mixture was evaporated *in vacuo*. The solid was resuspended in Et_2O, and the solvent decanted off to give a white solid. The product was carried forward without further purification.

2-Amino-1-[4-(1-adamantanecarbonyl)-1-piperazinyl] ethanone hydrochloride (18a). Following **GP7**, from 150 mg (0.370 mmol) **14a**, collected 75 mg of product.

3-Amino-1-[4-(1-adamantanecarbonyl)-1-piperazinyl] propanone hydrochloride (18b). Following **GP7**, from 160 mg (0.381 mmol) **14b**, collected 114 mg of product.

4-Amino-1-[4-(1-adamantanecarbonyl)-1-piperazinyl] butanone hydrochloride (18c). Following **GP7**, from 100 mg (0.231 mmol) **14c**, collected 59 mg of product.

5-Amino-1-[4-(1-adamantanecarbonyl)-1-piperazinyl]pentanone hydrochloride (18d). Following **GP7**, from 140 mg (0.313 mmol) **14d**, collected 119 mg of product.

6-Amino-1-[4-(1-adamantanecarbonyl)-1-piperazinyl] hexanone hydrochloride (18e). Following **GP7**, from 120 mg (0.260 mmol) **14e**, collected 99 mg of product.

2-Amino-1-[4-[[5-(dimethylamino)-1-naphthalenyl] sulfonyl]-1-piperazinyl]ethanone (19a). Following **GP7**, from 249 mg (0.522 mmol) **15a**, collected 284 mg of product.

3-Amino-1-[4-[[5-(dimethylamino)-1-naphthalenyl] sulfonyl]-1-piperazinyl]propanone (19b). Following **GP7**, from 329 mg (0.671 mmol) **15b**, collected 197 mg of product.

4-Amino-1-[4-[[5-(dimethylamino)-1-naphthalenyl] sulfonyl]-1-piperazinyl]butanone (19c). Following **GP7**, from 150 mg (0.297 mmol) **15c**, collected 140 mg of product.

5-Amino-1-[4-[[5-(dimethylamino)-1-naphthalenyl] sulfonyl]-1-piperazinyl]pentanone (19d). Following **GP7**, from 154 mg (0.297 mmol) **15d**, collected 146 mg of product.

6-Amino-1-[4-[[5-(dimethylamino)-1-naphthalenyl] sulfonyl]-1-piperazinyl]hexanone (19e). Following **GP7**, from 158 mg (0.297 mmol) **15e**, collected 150 mg of product.

2-Amino-1-[4-(1-naphthalenecarbonyl)-1-piperazinyl] ethanone hydrochloride (20a). Following **GP7**, from 140 mg (0.352 mmol) **16a**, collected 114 mg of product.

3-Amino-1-[4-(1-naphthalenecarbonyl)-1-piperazinyl] propanone hydrochloride (20b). Following **GP7**, from 155 mg (0.377 mmol) **16b**, collected 127 mg of product.

4-Amino-1-[4-(1-naphthalenecarbonyl)-1-piperazinyl] butanone hydrochloride (20c). Following **GP7**, from 160 mg (0.376 mmol) **16c**, collected 134 mg of product.

5-Amino-1-[4-(1-naphthalenecarbonyl)-1-piperazinyl]pentanone hydrochloride (20d). Following **GP7**, from 120 mg (0.273 mmol) **16d**, collected 99 mg of product.

6-Amino-1-[4-(1-naphthalenecarbonyl)-1-piperazinyl] hexanone hydrochloride (20e). Following **GP7**, from 170 mg (0.375 mmol) **16e**, collected 141 mg of product.

2-Amino-1-[4-(1-naphthalenesulfonyl)-1-piperazinyl] ethanone hydrochloride (21a). Following **GP7**, from (140 mg, 0.323 mmol) **17a**, collected 120 mg of product.

General procedure for the synthesis of compounds 22a–e (GP8). Compound **18** (1 equiv.) and DIPEA (3 equiv.) were stirred in DCM (~0.05 M relative to **18**). Once fully dissolved, acryloyl chloride (1.1 equiv.) was added. Upon completion by thin layer chromatography, the reaction mixture was evaporated *in vacuo*. **22a–e** were purified as specified for each compound below.

***N*-2-[4-[[1-Adamantanecarbonyl]-1-piperazinyl]-2-oxoethyl] propenamide (22a).** The residue obtained following setup according to **GP8** was redissolved in water (~10 mL) and EtOAc (~10 mL). Following phase separation, the aqueous phase was extracted with EtOAc, then the organic phases were combined and washed with saturated $NaHCO_3$ (2 × 10 mL) and brine (2 × 10 mL). The organic phase was collected, dried over $MgSO_4$, and evaporated under vacuum to give a white, microcrystalline solid. From 50 mg (0.146 mmol) of starting amine **18a**, recovered 13 mg (25%) of product. ^{1}H NMR (400 MHz, $CDCl_3$) δ 6.74 (br. s, 1H), 6.31 (dd, J = 1.3, 17.0 Hz, 1H), 6.19 (dd, J = 10.1, 17.0 Hz, 1H), 5.67 (dd, J = 1.1, 10.1 Hz, 1H), 4.15 (d, J = 4.1 Hz, 2H), 3.72 (m, 4H), 3.63 (m, 2H), 3.43 (m, 2H), 2.05 (s, 3H), 1.98 (m, 6H), 1.72 (m, 6H). ^{13}C NMR (101 MHz, $CDCl_3$) δ 176.22, 166.84, 165.51, 130.39, 127.10, 45.25, 44.87, 44.68, 42.36, 41.89, 41.40, 39.18, 36.64, 28.47. HRMS (ESI) calc'd for $C_{20}H_{29}N_3O_3Na$ ($[MNa]^+$): 382.2107, found: 382.2109.

***N*-3-[4-[[1-Adamantanecarbonyl]-1-piperazinyl]-3-oxopropyl] propenamide (22b).** The solid obtained following setup according to **GP8** was resuspended in water and crushed to give a fine powder. The powder was collected by filtration and dried under vacuum. From 100 mg (0.281 mmol) of **18b**, recovered 50 mg (48%) of product. ^{1}H NMR (400 MHz, $CDCl_3$) δ 6.49 (br. s, 1H), 6.26 (d, J = 17.0 Hz, 1H), 6.06 (dd, J = 10.3, 17.0 Hz, 1H), 5.62 (d, J = 10.3 Hz, 1H), 3.63 (m, 8H (several overlapping signals)), 3.41 (m, 2H), 2.57 (t, J = 5.5 Hz, 1H), 2.05 (s, 3H), 1.98 (m, 6H), 1.72 (m, 6H). ^{13}C NMR (101 MHz, $CDCl_3$) δ 176.21, 170.52, 165.61, 131.04, 126.56, 45.46, 45.35, 44.99, 41.89, 41.85, 39.18, 36.66, 35.11, 32.97, 28.50. HRMS (ESI) calc'd for $C_{21}H_{31}N_3O_3Na$ ($[MNa]^+$): 396.2263, found: 396.2261.

***N*-4-[4-[[1-Adamantanecarbonyl]-1-piperazinyl]-4-oxobutyl] propenamide (22c).** The residue obtained following setup according to **GP8** was diluted in DCM (~15 mL) and washed with water (~10 mL) and saturated $NaHCO_3$ (2 × 10 mL). The organic phase was dried over $MgSO_4$ and evaporated under vacuum to give a white solid. From 50 mg (0.135 mmol) of **18c**, recovered 19 mg (36%). ^{1}H NMR (400 MHz, $CDCl_3$) δ 6.44 (br. s, 1H), 6.24 (dd, J = 1.5, 17.0 Hz, 1H), 6.08 (dd, J = 10.2, 17.0 Hz, 1H), 5.61 (dd, J = 1.5, 10.2 Hz, 1H), 3.67 (m, 4H), 3.59 (m, 2H), 3.44 (m, 1H), 3.38 (q, J = 6.2 Hz, 2H), 2.42 (t, J = 6.7 Hz, 2H), 2.04 (s, 3H), 1.97 (m, 6H), 1.91 (qu, J = 6.6 Hz, 2H), 1.72 (m, 6H). ^{13}C NMR (101 MHz, $CDCl_3$) δ 176.18, 171.72, 165.84, 131.19, 126.17, 45.70, 45.42, 45.00, 42.01, 41.86, 39.64, 39.17, 36.66, 31.15, 28.49, 24.26. HRMS (ESI) calc'd for $C_{22}H_{33}N_3O_3Na$ ($[MNa]^+$): 410.2420, found: 410.2399.

***N*-5-[4-[[1-Adamantanecarbonyl]-1-piperazinyl]-5-oxopentyl] propenamide (22d).** The residue obtained following setup according to **GP8** was redissolved in EtOAc (20 mL) and washed with saturated $NaHCO_3$ (2 × 10 mL), water (2 × 10 mL) and brine (2 × 10 mL). The organic phase was dried over $MgSO_4$ and evaporated. The resulting solid was triturated with Et_2O, which was then decanted off. The solid was washed once with pentane, then dried, to give a white powder. From 100 mg (0.260 mmol) of **18d**, recovered 31 mg (30%) of product. ^{1}H NMR (400 MHz, $CDCl_3$) δ 6.27 (dd, J = 1.5, 17.0 Hz, 1H), 6.10 (dd, J = 10.2, 17.0 Hz, 2H, overlaps with NH signal), 5.62 (dd, J = 1.5, 10.2 Hz, 1H), 3.69 (m, 4H), 3.60 (m, 2H), 3.45 (m, 2H), 3.35 (q, J = 6.3 Hz, 2H), 2.38 (t, J = 7.1 Hz, 2H), 2.05 (s, 3H), 1.98 (m, 6H), 1.70 (m, 8H (2 overlapping signals)), 1.61 (m, 2H). ^{13}C NMR (101 MHz, $CDCl_3$) δ 176.24, 171.70, 165.81, 131.10, 126.32, 45.69, 45.58, 45.07, 41.96, 41.89, 39.19, 39.11, 36.68, 32.52, 28.96, 28.51, 22.06. HRMS (ESI) calc'd for $C_{23}H_{35}N_3O_3Na$ ($[MNa]^+$): 424.2576, found: 424.2590.

***N*-6-[4-[[1-Adamantanecarbonyl]-1-piperazinyl]-6-oxohexyl] propenamide (22e).** The residue obtained following setup according to **GP8** was redissolved in EtOAc (20 mL) and washed with saturated $NaHCO_3$ (2 × 10 mL), water (2 × 10 mL) and brine (2 × 10 mL). The organic phase was dried over $MgSO_4$ and evaporated, then was purified by preparative thin layer chromatography (5% MeOH in DCM) to give a white solid. From 90 mg (0.226 mmol) of **18e**, recovered 8 mg (9%) of product. ^{1}H NMR (400 MHz, $CDCl_3$) δ 6.27 (dd, J = 1.5, 17.0 Hz, 1H), 6.10 (dd, J = 10.2, 17.0 Hz, 1H), 5.96 (br. s, 1H), 5.62 (dd, J = 1.5, 10.2 Hz, 1H), 3.68 (m, 4H), 3.60 (m, 2H), 3.45 (m, 2H), 3.35 (q, J = 6.6 Hz, 2H), 2.34 (t, J = 7.3 Hz, 2H), 2.05 (s, 3H), 1.98 (m, 6H), 1.73 (t, J = 13.4 Hz, 1H), 1.66 (m, 8H, 2 overlapping signals, overlaps with water resonance), 1.57 (qu, J = 7.2 Hz, 2H), 1.39 (m, 2H). ^{13}C NMR (101 MHz, $CDCl_3$) δ 176.24, 171.79, 165.71, 131.12, 126.32, 45.71, 45.65, 45.04, 41.89, 39.19 (2 overlapping signals), 36.69, 33.01, 29.15, 28.52, 26.55, 24.39. HRMS (ESI) calc'd for $C_{24}H_{37}N_3O_3$-Na ($[MNa]^+$): 438.2733, found: 438.2738.

***N*-2-[4-[[5-(Dimethylamino)-1-naphthalenyl]sulfonyl]-1-piperazinyl]-2-oxoethylpropenamide (23a).** Compound **19a** (0.2116 g, 0.603 mmol) was dissolved in DCM (5 mL). DIPEA (259 μL, 1.49 mmol), and acryloyl chloride (80 μL, 0.784 mmol) were added and the reaction mixture was stirred overnight. The solvent was removed *in vacuo* and the residue redissolved in ethyl acetate (10 mL). The solution was washed with saturated aqueous bicarbonate (15 mL) and brine (15 mL) and dried over $MgSO_4$. The solvent was removed *in vacuo*, and the yellowish oil like products were purified using flash chromatography (solvent system 2) to give the product as a yellow crystalline solid (46 mg, 51%). ^{1}H NMR (400 MHz, $CDCl_3$) δ 8.60 (d, J = 8.5 Hz, 1H), 8.36 (d, J = 8.6 Hz, 1H), 8.21 (dd, J = 1.2, 7.4 Hz, 1H), 7.55 (t, J = 8.2 Hz, 2H), 7.20 (d, J = 7.5 Hz, 1H), 6.59 (br. s, 1H), 6.27 (dd, J = 1.5, 17.0 Hz, 1H), 6.13 (dd, J = 10.2, 17.0 Hz, 1H), 5.65 (dd, J = 1.5, 10.2 Hz, 1H), 4.05 (d, J = 4.1 Hz, 2H), 3.68 (t, J = 5.1 Hz, 2H), 3.47 (m, 2H), 3.21 (m, 4H), 2.90 (s, 6H). ^{13}C NMR (101 MHz, $CDCl_3$) δ 166.42, 165.37, 132.06, 131.22, 130.97, 130.31, 130.19, 128.39, 127.09, 123.31, 119.38, 115.54, 45.50, 45.31, 44.16, 41.66, 41.19. HRMS (ESI) calc'd for $C_{21}H_{26}N_4O_4SNa$ ([MNa]$^+$): 453.1572, found: 453.1570.

***N*-3-[4-[[5-(Dimethylamino)-1-naphthalenyl]sulfonyl]-1-piperazinyl]-3-oxopropylpropenamide (23b).** Compound **19b** (0.1537 g, 0.421 mmol) were dissolved in DCM. DIPEA (188 μL, 1.08 mmol), and acryloyl chloride (52 μL, 0.51 mmol) were added and left to stir overnight. The solvent was removed *in vacuo* and the residue redissolved in ethyl acetate (10 mL). The solution was washed with saturated aqueous bicarbonate (15 mL) and brine (15 mL) and dried over $MgSO_4$. The solvent was removed *in vacuo*, and the yellowish oil like products were purified using flash chromatography (solvent system 2) to give the product as a yellow residue (77 mg, 41%). ^{1}H NMR (400 MHz, $CDCl_3$) δ 8.56 (d, J = 8.5 Hz, 1H), 8.34 (d, J = 8.7 Hz, 1H), 8.18 (dd, J = 1.2, 7.4 Hz, 1H), 7.52 (t, J = 7.9 Hz, 2H), 7.17 (d, J = 7.2 Hz, 1H), 6.44 (br. s, 1H), 6.19 (dd, J = 1.4, 17.0 Hz, 1H), 5.99 (dd, J = 10.2, 17.0 Hz, 1H), 5.55 (dd, J = 1.5, 10.3 Hz, 1H), 3.61 (m, 2H), 3.53 (m, 2H), 3.44 (t, J = 5.2 Hz, 2H), 3.16 (m, 4H), 2.87 (s, 6H), 2.46 (t, J = 5.7 Hz, 2H). ^{13}C NMR (101 MHz, $CDCl_3$) δ 170.15, 165.57, 152.02, 132.31, 131.21, 130.99, 130.92, 130.42, 130.21, 128.40, 126.40, 123.28, 119.39, 115.50, 45.65, 45.51, 45.46, 44.97, 41.15, 35.05, 32.81. HRMS (ESI) calc'd for $C_{22}H_{28}N_4O_4SNa$ ([MNa]$^+$): 467.1729, found: 467.1716.

General procedure for the preparation of compounds 23c–e (GP9). Compound **19c–e** (0.293 mmol), acryloyl chloride (26 μL, 0.322 mmol), and DIPEA (153 μL, 0.879 mmol) were stirred in DCM (6 mL). The reaction was complete by TLC analysis (10% MeOH in DCM) after 1 h. The solvent was removed *in vacuo*, then the material was redissolved in EtOAc (20 mL) and washed with water (10 mL), saturated $NaHCO_3$ (10 mL) and brine (10 mL). The organic phase was collected, dried over $MgSO_4$, and evaporated *in vacuo*. The residue was triturated with Et_2O and the solvent decanted off, then the resulting solid was washed several times with Et_2O, and dried under high vacuum to give the product as a crunchy yellow foam.

***N*-4-[4-[[5-(Dimethylamino)-1-naphthalenyl]sulfonyl]-1-piperazinyl]-4-oxobutylpropenamide (23c).** Following **GP9**, collected 67 mg/50% of product. ^{1}H NMR (400 MHz, $CDCl_3$) δ 8.59 (d, J = 8.5 Hz, 1H), 8.36 (d, J = 8.7 Hz, 1H), 8.20 (dd, J = 1.2, 7.3 Hz, 1H), 7.54 (dd, J = 7.6, 8.5 Hz, 2H), 7.19 (d, J = 7.5 Hz, 1H), 6.22 (br. s, 1H), 6.14 (dd, J = 1.5, 17.0 Hz, 1H), 5.99 (dd, J = 10.2, 17.0 Hz, 1H), 5.52 (dd, J = 1.5, 10.2 Hz, 1H), 3.64 (t, J = 5.0 Hz, 1H), 3.48 (m, 2H), 3.32 (q, J = 6.2 Hz, 2H), 3.17 (m, 4H), 2.89 (s, 6H), 2.32 (t, J = 6.7 Hz, 2H), 1.84 (qu, J = 6.6 Hz, 2H). ^{13}C NMR (101 MHz, $CDCl_3$) δ 171.39, 165.78, 151.96, 132.36, 131.20, 131.09, 130.95, 130.45, 130.20, 128.41, 126.21, 123.36, 119.50, 115.54, 45.70, 45.57, 45.52, 45.24, 41.35, 39.52, 30.97, 24.19. HRMS (ESI) calc'd for $C_{23}H_{30}N_4O_4SNa$ ([MNa]$^+$): 481.1885, found: 481.1878.

***N*-5-[4-[[5-(Dimethylamino)-1-naphthalenyl]sulfonyl]-1-piperazinyl]-5-oxopentylpropenamide (23d).** Following **GP9**, collected 74 mg/53% of product. ^{1}H NMR (400 MHz, $CDCl_3$) δ 8.59 (d, J = 8.6 Hz, 1H), 8.37 (d, J = 8.6 Hz, 1H), 8.20 (dd, J = 1.2, 7.3 Hz, 1H), 7.55 (dd, J = 7.5, 8.6 Hz, 2H), 7.20 (d, J = 7.5 Hz, 1H), 6.24 (dd, J = 1.5, 17.0 Hz, 1H), 6.05 (dd, J = 10.3, 17.0 Hz, 1H), 5.97 (br. s, 1H), 5.60 (dd, J = 1.5, 10.3 Hz, 1H), 3.64 (t, J = 5.0 Hz, 2H), 3.49 (m, 2H), 3.29 (q, J = 6.3 Hz, 2H), 3.17 (m, 4H), 2.89 (s, 6H), 2.27 (t, J = 7.0 Hz, 2H), 1.58 (m, 4H (overlaps with HOD)). ^{13}C NMR (101 MHz, $CDCl_3$) δ 171.39, 165.83, 151.97, 132.31, 131.21, 131.03, 130.96, 130.44, 130.20, 128.41, 126.34, 123.33, 119.46, 115.51, 45.79, 45.56, 45.20, 41.25, 39.02, 32.37, 28.86, 21.92. HRMS (ESI) calc'd for $C_{24}H_{32}N_4O_4SNa$ ([MNa]$^+$): 495.2042, found: 495.2056.

***N*-6-[4-[[5-(Dimethylamino)-1-naphthalenyl]sulfonyl]-1-piperazinyl]-6-oxohexylpropenamide (23d).** Following **GP9**, collected 81 mg/57% of product. ^{1}H NMR (400 MHz, $CDCl_3$) δ 8.59 (d, J = 8.4 Hz, 1H), 8.38 (d, J = 8.6 Hz, 1H), 8.20 (dd, J = 1.1, 7.3 Hz, 1H), 7.55 (dd, J = 7.6, 8.5 Hz, 2H), 7.19 (d, J = 7.4 Hz, 1H), 6.25 (dd, J = 1.5, 17.0 Hz, 1H), 6.06 (dd, J = 10.2, 17.0 Hz, 1H), 5.82 (br. s, 1H), 5.60 (dd, J = 1.5, 10.2 Hz, 1H), 3.64 (t, J = 4.9 Hz, 2H), 3.49 (t, J = 4.8 Hz, 2H), 3.31 (q, J = 6.6 Hz, 2H), 3.17 (m, 4H), 2.89 (s, 6H), 2.24 (t, J = 7.3 Hz, 2H), 1.55 (m, 4H (overlaps with HOD)), 1.31 (m, 2H). ^{13}C NMR (101 MHz, $CDCl_3$) δ 171.45, 165.71, 151.97, 132.33, 131.19, 131.07, 130.95, 130.45, 130.20, 128.39, 126.32, 123.32, 119.48, 115.51, 45.78, 45.56, 45.22, 41.19, 39.15, 32.88, 29.10, 26.47, 24.28. HRMS (ESI) calc'd for $C_{25}H_{34}N_4O_4SNa$ ([MNa]$^+$): 509.2198, found: 509.2182.

General procedure for the synthesis of compounds 24a–e (GP10). Compound **20a–e** (0.240 mmol) and DIPEA (125 μL, 0.720 mmol) were stirred in DCM (5 mL) at R.T. Acryloyl chloride (21 μL, 0.264 mmol) was added, and the reaction mixture was stirred for 5 min, upon which it was determined to be complete by TLC analysis (TLC solvent system 2). The reaction mixture was concentrated *in vacuo*, then the residue redissolved in EtOAc (25 mL). The organic phase was washed with 5% AcOH (15 mL) then sat. $NaHCO_3$ (15 mL), then brine (15 mL). The organic phase was dried over $MgSO_4$ and evaporated under reduced pressure. The residue was adsorbed onto Celite® and purified by flash chromatography (0–5% MeOH in 1 : 1 DCM/hexanes). Fractions containing

product were collected, and solvent removed *in vacuo* to give a white foam.

***N*-2-[4-[[1-Naphthalenecarbonyl]-1-piperazinyl]-2-oxoethyl] propenamide (24a).** Following **GP10**, collected 46 mg/55% of product. ^{1}H NMR (400 MHz, $CDCl_3$) δ 7.91 (m, 2H), 7.81 (m, 1H), 7.52 (m, 3H), 7.42 (d, J = 6.0 Hz, 1H), 6.66 (s, 1H), 6.31 (m, 1H), 6.18 (m, 2 overlapping doublets, 1H), 5.68 (d, J = 10.6 Hz, 1H), 4.22–3.20 (m, 10H). ^{13}C NMR (101 MHz, $CDCl_3$) δ 169.85 (determined by HMBC), 166.79, 165.39, 133.55, 133.23, 130.26, 129.71, 129.51, 128.67, 127.33, 127.00, 126.70, 125.19, 124.39, 123.99, 46.77 (rotamers, 1C), 44.66 (rotamers, 1C), 42.51, 42.02, 41.45 (rotamers, 1C). HRMS (ESI) calc'd for $C_{20}H_{21}N_3O_3Na$ ($[MNa]^+$): 374.1481, found: 374.1507.

***N*-3-[4-[[1-Naphthalenecarbonyl]-1-piperazinyl]-3-oxopropyl] propenamide (24b).** Following **GP10**, collected 53 mg/60% of product. ^{1}H NMR (400 MHz, $CDCl_3$) δ 7.90 (m, 2H), 7.81 (m, 1H), 7.52 (m, 3H), 7.42 (d, J = 7.1 Hz, 1H), 6.40 (s, 1H), 6.26 (m, 1H), 6.05 (2 overlapping doublets, J = 10.3, 17.0 Hz, 1H), 5.62 (d, J = 10.2 Hz, 1H), 4.07–3.14 (m, 10H), 2.64 (t, J = 5.2 Hz, 1H), 2.49 (br. s, 1H). ^{13}C NMR (101 MHz, $CDCl_3$) δ 170.55 (determined by HMBC), 169.73 (determined by HMBC), 165.47, 133.53, 130.90, 129.62, 129.53, 128.64, 127.27, 126.66, 126.43, 125.19, 124.44, 123.96, 46.79, 45.69, 45.16, 41.74 (rotamers, 1C), 34.98, 32.88. HRMS (ESI) calc'd for $C_{21}H_{23}N_3O_3Na$ ($[MNa]^+$): 388.1638, found: 388.1614.

***N*-4-[4-[[1-Naphthalenecarbonyl]-1-piperazinyl]-4-oxobutyl] propenamide (24c).** Following **GP10**, collected 37 mg/41% of product. ^{1}H NMR (400 MHz, $CDCl_3$) δ 7.90 (m, 2H), 7.81 (m, 1H), 7.52 (m, 3H), 7.42 (d, J = 6.9 Hz, 1H), 6.24 (m, 2H), 6.06 (2 overlapping doublets, J = 9.1 Hz, 1H), 5.61 (d, J = 9.9 Hz, 1H), 4.06–3.14 (m, 10H), 2.49 (t, J = 6.3 Hz, 1H), 2.33 (br. s, 1H), 1.93 (m, 2H). ^{13}C NMR (101 MHz, $CDCl_3$) δ 171.34 (determined by HMBC), 169.37 (determined by HMBC), 165.65 (determined by HMBC), 133.53, 131.08, 129.59, 129.53, 128.62, 127.26, 126.64, 126.07, 125.19, 124.47, 123.95, 46.87 (determined by HMBC), 45.42, 41.73, 41.62 (rotamers, determined by HMBC), 39.52, 31.03, 24.18. HRMS (ESI) calc'd for $C_{22}H_{25}N_3O_3Na$ ($[MNa]^+$): 402.1794, found: 402.1792.

***N*-5-[4-[[1-Naphthalenecarbonyl]-1-piperazinyl]-5-oxopentyl] propenamide (24d).** Following **GP10**, collected 56 mg/60% of product. ^{1}H NMR (400 MHz, $CDCl_3$) δ 7.90 (m, 2H), 7.81 (m, 1H), 7.51 (m, 3H), 7.42 (d, J = 6.8 Hz, 1H), 6.24 (m, 1H), 6.05 (m, 2H), 5.59 (m, 1H), 4.05–3.14 (m, 10H), 2.43 (t, J = 6.3 Hz, 1H), 2.28 (br. s, 1H), 1.64 (m, 4H). ^{13}C NMR (101 MHz, $CDCl_3$) δ 171.50, 169.76, 165.62, 133.53, 130.97, 129.57, 129.53, 128.61, 127.25, 126.64, 126.13, 125.19, 124.48, 123.94, 47.06 (rotamers, 1C), 45.36, 41.99 (rotamers, 1C), 41.56, 38.98, 32.41, 28.89, 21.91. HRMS (ESI) calc'd for $C_{23}H_{27}N_3O_3Na$ ($[MNa]^+$): 416.1950, found: 416.1935.

***N*-6-[4-[[1-Naphthalenecarbonyl]-1-piperazinyl]-6-oxohexyl] propenamide (24e).** Following **GP10**, collected 66 mg/67% of product. ^{1}H NMR (400 MHz, $CDCl_3$) δ 7.90 (m, 2H), 7.82 (m, 1H), 7.51 (m, 3H), 7.42 (d, J = 6.8 Hz, 1H), 6.25 (m, 1H), 6.07 (2 overlapping doublets, J = 9.1 Hz, 1H), 5.89 (s, 1H), 5.60 (dd, J = 1.4, 10.2 Hz, 1H), 4.08–3.12 (m, 10H), 2.40 (t, J = 6.5 Hz, 1H), 2.25 (br. s, 1H), 1.59 (m, 4H), 1.37 (m, 2H). ^{13}C NMR (101 MHz, $CDCl_3$) δ 171.61, 169.80 (determined by HSQC), 165.54, 133.53, 131.00, 129.55 (2 overlapping signals, 2C), 128.61, 127.25, 126.63, 126.11, 125.19, 124.49, 123.94, 47.06 (rotamers, 1C), 45.96, 45.38, 41.98 (rotamers, 1C), 39.04, 32.89, 29.06, 26.41, 24.27. HRMS (ESI) calc'd for $C_{24}H_{29}N_3O_3Na$ ($[MNa]^+$): 430.2107, found: 430.2093.

***N*-2-[4-[[1-Naphthalenylsulfonyl]-1-piperazinyl]-2-oxoethyl] propenamide (25a).** To a stirred solution of **21a** (100 mg, 0.270 mmol) and DIPEA (141 μL, 0.814 mmol) was added acryloyl chloride (24 μL, 0.297 mmol). The reaction was complete by TLC analysis (10% MeOH in DCM) after 3 h. The reaction solvent was removed *in vacuo*, then the residue washed with Et_2O and dried under vacuum. The residue was then redissolved in EtOAc (20 mL) and washed with H_2O (20 mL) and brine (20 mL). The organic material was dried over $MgSO_4$ and evaporated. The residue was triturated with Et_2O, then the solvent was decanted off and the product dried under vacuum to give a white solid (78 mg, 74%). ^{1}H NMR (400 MHz, $CDCl_3$) δ 8.71 (d, J = 8.5 Hz, 1H), 8.21 (d, J = 7.3 Hz, 1H), 8.11 (d, J = 8.1 Hz, 1H), 7.95 (d, J = 8.0 Hz, 1H), 7.62 (m, 3H), 6.60 (s, 1H), 6.26 (dd, J = 1.1, 16.9 Hz, 1H), 6.13 (dd, J = 10.2, 17.0 Hz, 1H), 5.64 (dd, J = 1.2, 10.2 Hz, 1H), 4.04 (d, J = 4.1 Hz, 2H), 3.68 (t, J = 4.9 Hz, 2H), 3.47 (t, J = 4.9 Hz, 2H), 3.20 (m, 4H). ^{13}C NMR (101 MHz, $CDCl_3$) δ 166.53, 165.45, 135.16, 134.54, 131.94, 131.01, 130.28, 129.26, 128.94, 128.56, 127.23, 127.17, 124.89, 124.33, 45.58, 45.42, 44.22, 41.71, 41.27. HRMS (ESI) calc'd for $C_{19}H_{21}N_3O_4SNa$ ($[MNa]^+$): 410.1150, found: 410.1126.

TG2 inhibition assay

Recombinant TG2 was expressed and purified from *E. coli* as previously described.[50] TG2 activity was determined according to a previously published colorimetric activity assay using the chromogenic substrate Cbz-Glu(γ-*p*-nitrophenyl ester)Gly (AL5).[36] In order to determine irreversible inhibition parameters for each inhibitor, enzymatic assays were run under Kitz and Wilson conditions, in the presence of 100 μM AL5 substrate, in triplicate.[51] Buffered solutions of 50 mM of 3-(4-morpholino)propanesulfonic acid (MOPS) (pH 6.9), 7.5 mM $CaCl_2$, 100 μM AL5, and various concentrations of inhibitor (from 0.5 to 900 μM, depending on the inhibitor) were prepared in a 96-well polystyrene microplate with a final volume of 200 μL at 25 °C. AL5 and inhibitor stocks were prepared in DMSO ensuring that the final concentration of this co-solvent did not exceed 5% v/v. If necessary, working stocks of each inhibitor were diluted with water to maintain less than 5% v/v DMSO. To initiate the enzymatic reaction, 5 mU mL^{-1} TG2, or water for the blank, was added to the well and the formation of the hydrolysis product, *p*-nitrophenolate, was followed at 405 nm for 20 min using a BioTek Synergy 4 plate reader. Observed first-order rate constants of inactivation (k_{obs}) were obtained by fitting the inhibition data sets with non-linear regression to mono-exponential eqn (1) using GraphPad Prism software.

$$Abs_t = Abs_{max} \times (1 - e^{-k_{obs}t}) \quad (1)$$

The rate constants measured at different inhibitor concentrations were then fitted by non-linear regression to a saturation kinetics model, using eqn (2).[52]

$$k_{obs} = \frac{k_{inact} \cdot [I]}{[I] + K_I \cdot \alpha} \quad (2)$$

In order to correct for the competition with the assay substrate, AL5, the inhibitor concentrations were divided by α, which equals $1 + [S]/K_M$, where K_M = 10 μM.[26] Inhibition parameters, k_{inact} and K_I, were then extrapolated from the fitting. If saturation with the inhibitor was not achieved, the observed rate constants were analyzed using double reciprocal fitting.

GTP binding assay

GTP binding was measured using a method reported previously.[26] TG2 (10 μg) was incubated at 25 °C for 30 min with or without irreversible inhibitor (at a concentration of 2 × K_I) with 3.0 mM $CaCl_2$ in 100 mM MOPS (pH = 6.54). The buffer was then exchanged to 100 mM MOPS (pH = 7.0), 1 mM EGTA, and 5 mM $MgCl_2$ to remove calcium using a 10 kDa molecular weight cut off membrane (Amicon tube). The fluorescent, nonhydrolyzable GTP analogue BODIPY GTP-γ-S (purchased from Invitrogen), whose fluorescence increases when bound to the protein, was then added to give a final concentration of 3.0 μM, and fluorescence was then measured on a microplate reader after 10 min of incubation (Ex/Em: 490/520 nm).

Protein and ligand preparation for molecular modelling

Two crystals were selected as a target receptor enzyme, and were imported from their PDB files, namely 2Q3Z and 3S3J. The structure was prepared using the preparation tool from MOE. First, water molecules, salts and ions were removed from the structure. All hydrogen atoms were then added (electrostatics: $1/r^2$, dielectric: 2, solvent: 80, van der Waals: 12–6) and the protein structures were finally verified, and corrected manually, for any problems or warnings such as chain breaks, termini missing or unreasonable charges. Finally, the binding site was created *via* the site finder tool from MOE. Ligands were drawn in ChemDraw and imported to MOE; partial charges were calculated using a MMFF94x forcefield and the system was eventually minimized following a 0.0001 kcal mol^{-1} $Å^{-2}$ gradient. After solvation, minimization was repeated.

Molecular docking

The "compute" tool from MOE was used to perform docking analysis of each ligand one by one following both non-covalent and covalent approaches. For the non-covalent approach, ligand placement was achieved using the Triangle Matcher protocol (London dG) to produce 30 poses. In addition, a Rigid Receptor refinement protocol was performed (GBVI/WSA dG) and a total of 5 to 15 final poses were obtained. Finally, using the builder tool from MOE, the covalent bonds between residue CYS277 and the acrylamide warhead of the bound inhibitors were manually created, prior to minimization of the system (0.001 kcal mol^{-1} $Å^{-2}$). For the covalent approach, a covalent bond formation between CYS277 and the acrylamide warhead was required using the "1,4 Michael Mercapto Addition" reaction, and ligand placement was achieved using the Rigid Receptor (GBVI/WSA dG) protocol to produce 30 poses.

Conclusions

We designed a small library of inhibitors based on known hydrophobic ligands, a known warhead, and varying lengths of tethers. Most of these inhibitors were novel, whereas two members of our series (**22a** and **23a**) were first published by the Griffin group.[21] We used a rapid and direct chromogenic assay to measure the kinetic parameters k_{inact} and K_I for each of the inhibitors studied herein, allowing for the first time the direct comparison of all inhibitors. Notably, inhibitors **22a**, **23a** and **25a** were far superior to any others. Importantly, we also provided the first direct evidence for their ability to inhibit GTP binding, at least partially. Intriguingly, molecular modelling did not prove useful for guiding structure-based design, in that the results from the docking studies predicted the exact opposite trends of what we observed experimentally. This discrepancy suggests that different crystallographic structures, obtained with small molecule inhibitors, may reveal TG2 in a different conformation, providing a more appropriate starting point for the structure-based design of such inhibitors. In the meantime, kinetic studies such as those presented herein can provide the empirical data required to drive forward the design of next generation TG2 inhibitors.

List of abbreviations

Cmpd.	Compound
DCM	Dichloromethane
DIPEA	*N*,*N*-Diisopropylethylamine
HBTU	2-(1*H*-Benzotriazol-1-yl)-1,1,3,3-tetramethyluronium hexafluorophosphate
qu	Quintet (multiplicity)
TLC	Thin-layer chromatography

Conflicts of interest

There are no conflicts to declare.

Acknowledgements

JWK is grateful to the Natural Sciences and Engineering Research Council of Canada (NSERC) and the Canadian Institutes of Health Research (CIHR) for funding. AMMR also thanks NSERC for a CREATE graduate bursary.

Notes and references

1 S. Gundemir, G. Colak, J. Tucholski and G. V. Johnson, *Biochim. Biophys. Acta*, 2012, **1823**, 406.
2 R. L. Eckert, M. T. Kaartinen, M. Nurminskaya, A. M. Belkin, G. Colak, G. V. Johnson and K. Mehta, *Physiol. Rev.*, 2014, **94**, 383.
3 L. Lorand and R. M. Graham, *Nat. Rev. Mol. Cell Biol.*, 2003, **4**, 140.
4 W. P. Katt, M. A. Antonyak and R. A. Cerione, *Drug Discovery Today*, 2018, **23**, 575.
5 J. W. Keillor, C. M. Clouthier, K. Y. P. Apperley, A. Akbar and A. Mulani, *Bioorg. Chem.*, 2014, **57**, 186.
6 T. S. Johnson, M. Fisher, J. L. Haylor, Z. Hau, N. J. Skill, R. Jones, R. Saint, I. Coutts, M. E. Vickers, A. M. El Nahas and M. Griffin, *J. Am. Soc. Nephrol.*, 2007, **18**, 3078.
7 N. Shweke, N. Boulos, C. Jouanneau, S. Vandermeersch, G. Melino, J. C. Dussaule, C. Chatziantoniou, P. Ronco and J. J. Boffa, *Am. J. Pathol.*, 2008, **173**, 631.
8 M. C. W. Benn, W. Weber, E. Klotzsch, V. Vogel and S. A. Pot, *Curr. Opin. Biomed. Eng.*, 2019, **10**, 156.
9 W. Dieterich, T. Ehnis, M. Bauer, P. Donner, U. Volta, E. O. Riecken and D. Schuppan, *Nat. Med.*, 1997, **3**, 797.
10 D. Schuppan and W. Dieterich, *Chem. Biol.*, 2003, **10**, 199.
11 C. Tabolacci, A. De Martino, C. Mischiati, G. Feriotto and S. Beninati, *Med. Sci.*, 2019, **7**, 1–19.
12 M. L. Fisher, J. W. Keillor, W. Xu, R. L. Eckert and C. Kerr, *Mol. Cancer Res.*, 2015, **13**, 1083.
13 Z. Szondy, I. Korponay-Szabo, R. Kiraly, Z. Sarang and G. J. Tsay, *Biomedicine*, 2017, **7**, 15.
14 T. H. Jang, D. S. Lee, K. Choi, E. M. Jeong, I. G. Kim, Y. W. Kim, J. N. Chun, J. H. Jeon and H. H. Park, *PLoS One*, 2014, **9**, e107005.
15 N. S. Caron, L. N. Munsie, J. W. Keillor and R. Truant, *PLoS One*, 2012, **7**, e44159.
16 D. M. Pinkas, P. Strop, A. T. Brunger and C. Khosla, *PLoS Biol.*, 2007, **5**, e327.
17 J. W. Keillor and G. V. W. Johnson, *Expert Opin. Ther. Targets*, 2021, **25**, 721.
18 G. E. Begg, S. R. Holman, P. H. Stokes, J. M. Matthews, R. M. Graham and S. E. Iismaa, *J. Biol. Chem.*, 2006, **281**, 12603.
19 M. Song, H. Hwang, C. Y. Im and S. Y. Kim, *J. Med. Chem.*, 2017, **60**, 554.
20 E. A. Rorke, G. Adhikary, H. Szmacinski, J. R. Lakowicz, D. J. Weber, R. Godoy-Ruiz, P. Puranik, J. W. Keillor, E. W. J. Gates and R. L. Eckert, *Mol. Carcinog.*, 2022, **61**, 19.
21 E. Badarau, Z. Wang, D. L. Rathbone, A. Costanzi, T. Thibault, C. E. Murdoch, S. El Alaoui, M. Bartkeviciute and M. Griffin, *Chem. Biol.*, 2015, **22**, 1347.
22 J. Wityak, M. E. Prime, F. A. Brookfield, S. M. Courtney, S. Erfan, S. Johnsen, P. D. Johnson, M. Li, R. W. Marston, L. Reed, D. Vaidya, S. Schaertl, A. Pedret-Dunn, M. Beconi, D. Macdonald, I. Munoz-Sanjuan and C. Dominguez, *ACS Med. Chem. Lett.*, 2012, **3**, 1024.
23 S. Schaertl, M. Prime, J. Wityak, C. Dominguez, I. Munoz-Sanjuan, R. E. Pacifici, S. Courtney, A. Scheel and D. Macdonald, *J. Biomol. Screening*, 2010, **15**, 478.
24 C. Pardin, S. M. Gillet and J. W. Keillor, *Bioorg. Med. Chem.*, 2006, **14**, 8379.
25 J. W. Keillor and K. Y. Apperley, *Expert Opin. Ther. Pat.*, 2016, **26**, 49.
26 A. Akbar, N. M. R. McNeil, M. R. Albert, V. Ta, G. Adhikary, K. Bourgeois, R. L. Eckert and J. W. Keillor, *J. Med. Chem.*, 2017, **60**, 7910.
27 R. Wodtke, J. Wodtke, S. Hauser, M. Laube, D. Bauer, R. Rothe, C. Neuber, M. Pietsch, K. Kopka, J. Pietzsch and R. Loser, *J. Med. Chem.*, 2021, **64**, 3462.
28 P. de Macedo, C. Marrano and J. W. Keillor, *Bioorg. Med. Chem.*, 2002, **10**, 355.
29 C. Pardin, J. N. Pelletier, W. D. Lubell and J. W. Keillor, *J. Org. Chem.*, 2008, **73**, 5766.
30 D. Schuppan, M. Maki, K. E. A. Lundin, J. Isola, T. Friesing-Sosnik, J. Taavela, A. Popp, J. Koskenpato, J. Langhorst, O. Hovde, M. L. Lahdeaho, S. Fusco, M. Schumann, H. P. Torok, J. Kupcinskas, Y. Zopf, A. W. Lohse, M. Scheinin, K. Kull, L. Biedermann, V. Byrnes, A. Stallmach, J. Jahnsen, J. Zeitz, R. Mohrbacher, R. Greinwald and C. E. C. T. Group, *N. Engl. J. Med.*, 2021, **385**, 35.
31 D. Halim, K. Caron and J. W. Keillor, *Bioorg. Med. Chem. Lett.*, 2007, **17**, 305.
32 C. Marrano, P. de Macedo, P. Gagnon, D. Lapierre, C. Gravel and J. W. Keillor, *Bioorg. Med. Chem.*, 2001, **9**, 3231.
33 C. Marrano, P. de Macedo and J. W. Keillor, *Bioorg. Med. Chem.*, 2001, **9**, 1923.
34 M. R. Griffin, D. Rathbone and L. E. Badarau, WO2014057266A1, 2014.
35 C. P. Dominguez, M. Prime, R. Marston, F. A. Brookfield, S. M. Courtney, D. Macdonald, J. Wityak, C. J. Yarnold and D. Vaidya, WO2014047288A2, 2014.
36 A. Leblanc, C. Gravel, J. Labelle and J. W. Keillor, *Biochemistry*, 2001, **40**, 8335.
37 D. P. McEwen, K. R. Gee, H. C. Kang and R. R. Neubig, *Anal. Biochem.*, 2001, **291**, 109.
38 R. Wodtke, C. Hauser, G. Ruiz-Gomez, E. Jackel, D. Bauer, M. Lohse, A. Wong, J. Pufe, F. A. Ludwig, S. Fischer, S. Hauser, D. Greif, M. T. Pisabarro, J. Pietzsch, M. Pietsch and R. Löser, *J. Med. Chem.*, 2018, **61**, 4528.
39 N. Day and J. W. Keillor, *Anal. Biochem.*, 1999, **274**, 141.
40 K. E. Achyuthan and C. S. Greenberg, *J. Biol. Chem.*, 1987, **262**, 1901.
41 S. Seo, Y. Moon, J. Choi, S. Yoon, K. H. Jung, J. Cheon, W. Kim, D. Kim, C. H. Lee, S. W. Kim, K. S. Park and D. H. Lee, *Am. J. Cancer Res.*, 2019, **9**, 597.
42 J. Stamnaes, D. M. Pinkas, B. Fleckenstein, C. Khosla and L. M. Sollid, *J. Biol. Chem.*, 2010, **285**, 25402.
43 S. A. Attique, M. Hassan, M. Usman, R. M. Atif, S. Mahboob, K. A. Al-Ghanim, M. Bilal and M. Z. Nawaz, *Int. J. Environ. Res. Public Health*, 2019, **16**, 923.
44 N. S. Pagadala, K. Syed and J. Tuszynski, *Biophys. Rev.*, 2017, **9**, 91.
45 D. G. Alberg and S. L. Schreiber, *Science*, 1993, **262**, 248.
46 C. M. Clouthier, G. G. Mironov, V. Okhonin, M. V. Berezovski and J. W. Keillor, *Angew. Chem., Int. Ed.*, 2012, **51**, 12464.

47 G. G. Mironov, C. M. Clouthier, A. Akbar, J. W. Keillor and M. V. Berezovski, *Nat. Chem. Biol.*, 2016, **12**, 918.
48 C. Zhang, S. Wu, Z. Xi and L. Yi, *Tetrahedron*, 2017, **73**, 6651.
49 P. Vachal, J. M. Fletcher, T. M. Fong, C. C. Huang, J. Lao, J. C. Xiao, C. P. Shen, A. M. Strack, L. Shearman, S. Stribling, R. Z. Chen, A. Frassetto, X. Tong, J. Wang, R. G. Ball, N. N. Tsou, G. J. Hickey, D. F. Thompson, T. D. Faidley, S. Nicolich, J. Achanfuo-Yeboah, D. F. Hora, J. J. Hale and W. K. Hagmann, *J. Med. Chem.*, 2009, **52**, 2550.
50 I. Roy, O. Smith, C. M. Clouthier and J. W. Keillor, *Protein Expression Purif.*, 2013, **87**, 41.
51 R. Kitz and I. B. Wilson, *J. Biol. Chem.*, 1962, **237**, 3245.
52 S. R. Stone and J. Hofsteenge, *Biochem. J.*, 1985, **230**, 497.